AN1477

Digital Compensator Design for LLC Resonant Converter

*Author: Dhaval Patel and Ramesh Kankanala*
Microchip Technology Inc.

ABSTRACT

A half-bridge LLC resonant converter with Zero Voltage Switching (ZVS) and Pulse Frequency Modulation (PFM) is a widely used topology for DC/DC conversion. A Digital Signal Controller (DSC) provides component cost reduction, flexible design, and the ability to monitor and process the system conditions to achieve greater stability. The dynamics of the LLC resonant converter are investigated using the small signal modeling technique based on the Extended Describing Functions (EDF) methodology. A comprehensive description of compensator design for control of the LLC converter is also presented.

INTRODUCTION

The LLC resonant converter topology, illustrated in Figure 1, allows ZVS for half-bridge MOSFETs, thereby considerably lowering the switching losses and improving the converter efficiency. Mathematical modeling of resonant converters is different from the conventional fixed frequency Pulse-Width Modulation (PWM) converters. For LLC converter modeling, the method of averaging cannot be used because some state variables do not have a DC operating point. We should therefore, use other modeling techniques, such as the Extended Describing Function (EDF). In order to design a suitable digital compensator, the large signal and small signal models of the LLC resonant converter are derived using the EDF technique.

FIGURE 1:   LLC RESONANT CONVERTER SCHEMATIC

AN1477
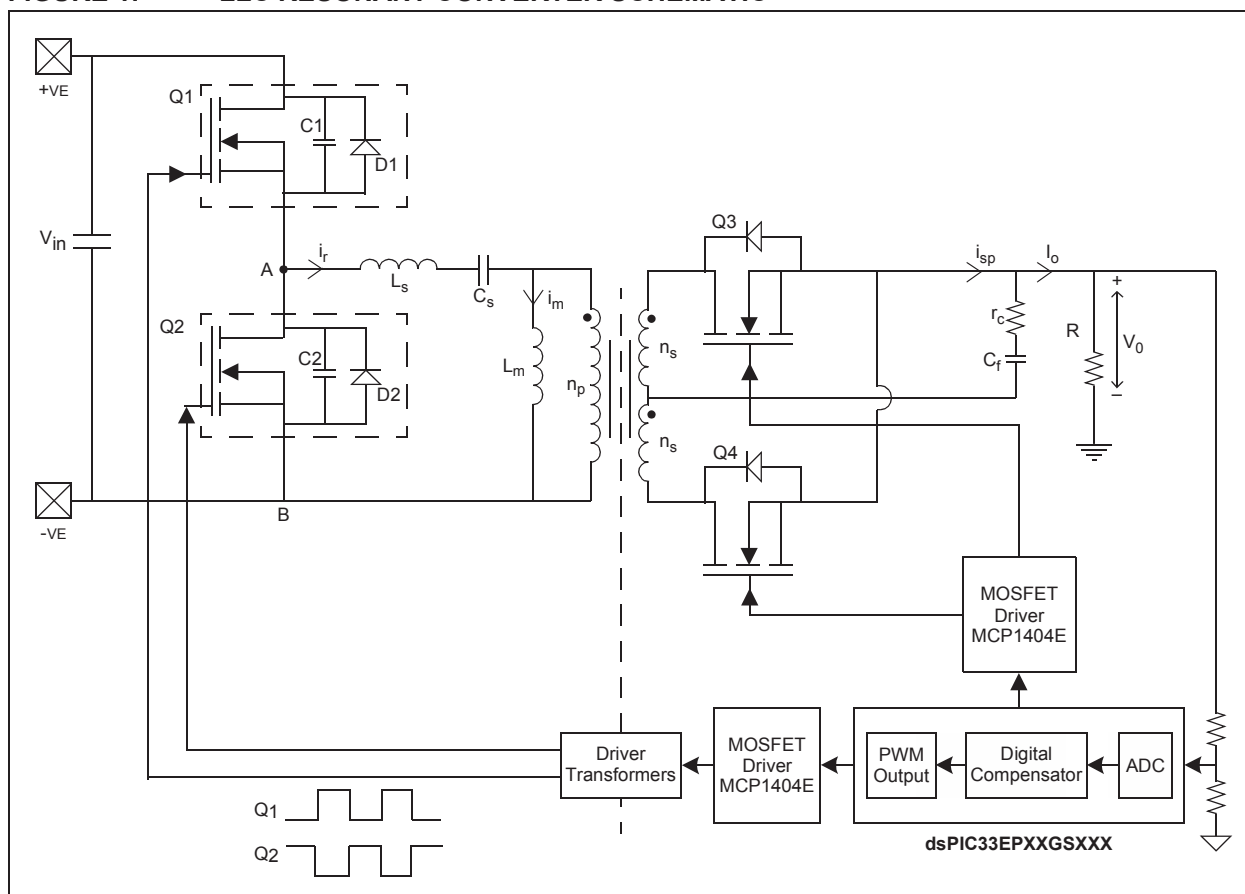
Conventional methods, such as State-Space Averaging (SSA), have been successfully applied to PWM switching converters. In PWM switching converters, the switch network is replaced by an average circuit model and only low-frequency (DC) components are considered, while ignoring switching harmonics. In general, the large and small signal modeling of PWM switching converters is done by considering the output LC filter. Typically, the natural frequency (f_O) of the output LC filter is much lower than the switching frequency (f_s).

In frequency controlled resonant converters, switching frequency is close to the natural frequency of the LC resonant tank. The inductor current and capacitor voltage of the LC resonant tank, magnetizing current and primary voltage of the transformer contain switching frequency harmonics, which must be considered to obtain an accurate model. Therefore, modeling is done by considering magnetizing inductance (L_m), leakage inductance (L_s) and resonant capacitance (C_s). The L_s, L_m and C_s constitute the primary resonant components.

The small signal modeling approach, based on the EDF method, is generally applied to model LLC resonant converters as this method considers all switching frequency harmonics for accuracy. Using the EDF, it is easy to obtain the commonly used transfer functions, such as control-to-output transfer function ($G_{v\omega}$) and line-to-output transfer function (G_{vg}).

SMALL SIGNAL MODELING OF LLC RESONANT CONVERTER

Resonant DC/DC converters are nonlinear systems and a dynamic model is helpful to determine the linearized small signal model, and thereby, the system transfer functions for the Pulse Frequency Modulated (PFM) DC/DC converters.

The following seven-step process describes how to obtain the plant transfer functions for the PFM DC/DC converters.

1. **Time Variant Nonlinear State Equations**

   State equations are obtained by writing the circuit equations using Kirchhoff's Laws for each state variable.

2. **Harmonic Approximation**

   Quasi-sinusoidal current and voltage waveforms of the LLC resonant tank are resonant current ($i_r(t)$), magnetizing current ($i_m(t)$) and voltage across resonant capacitor ($v_{Cr}(t)$). These parameters are approximated to their fundamental components. The current and voltage of the output filter are approximated to their DC components.

3. **Extended Describing Function (EDF)**

   A linear, stationary system responds to a sinusoid with another sinusoid of the same frequency, but with modified amplitude and phase. The describing function method is used to represent a nonlinear function in a linear manner by considering only the fundamental component of the response of the nonlinear system.

   In this application note, higher order harmonics are ignored as they are considered to be negligible. This principle of describing functions is extended to model resonant converters and it is labeled as EDF.

   Using the EDF method, the discontinuous terms in the nonlinear state equations are approximated to their fundamental or DC components.

4. **Harmonic Balance**

   The quasi-sinusoidal terms and the nonlinear discontinuous terms obtained from the harmonic approximation and EDF are substituted in the state equations. The coefficients of DC, sine and cosine components are then separated to obtain the modulation equations (an approximate large signal model).

5. **Obtaining the Steady-State Operating Point**

   A large signal model from the harmonic balance is used to obtain the steady-state operating point by setting the derivative terms of harmonic balance equations to zero. This is because the state variables do not change with time in steady state.

6. **Perturbation and Linearization of Harmonic Balance Equations**

   The large signal model obtained from the harmonic balance has nonlinear terms arising from the product of two or more time varying quantities. The linearized model is obtained by perturbing the large signal model equations about a chosen operating point and by eliminating the higher order (nonlinear) terms.

7. **State-Space Model**

   The state-space model of a continuous time dynamic system can be obtained from the perturbed and linearized model of the harmonic balance equations, described in Step 6, to derive the control-to-output transfer function.

Derivation of Nonlinear State Equations

A quasi-square wave voltage (v_{AB}), generated from the active half-bridge network, is applied to the resonant tank of the LLC resonant converter, as illustrated in Figure 2.

FIGURE 2: **EQUIVALENT CIRCUIT OF LLC RESONANT CONVERTER**
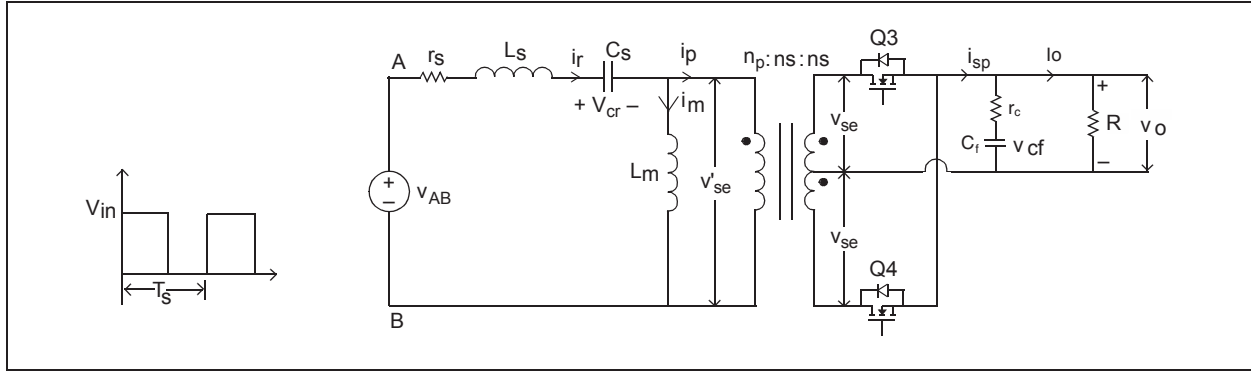
The state equations are obtained in Continuous Tank Current mode by using Kirchhoff's Current Law (KCL) and Kirchhoff's Voltage Law (KVL), as shown in Equation 1 through Equation 4.

EQUATION 1: **RESONANT TANK VOLTAGE**

$$v_{AB} = L_s\left(\frac{di_r}{dt}\right) + i_r r_s + v_{cr} + v'_{se}$$

Where:

$$v'_{se} = n\,v_{se}$$
$$= n \times \text{sgn}(i_p) \times abs(v_{se})$$
$$= n \times \text{sgn}(i_p) \times (r_d\,abs(i_{sp}) + v_o)$$

Here:

$$\text{sgn}(i_p) = \{-1,\ if\,i_p < 0$$
$$+1,\ if\,i_p \geq 0\}$$

In this application, the LLC resonant converter output voltage is regulated by modulating the switching frequency (ω_s).

EQUATION 2: **RESONANT TANK CURRENT**

$$i_r = C_s\frac{dv_{cr}}{dt}$$

EQUATION 3: **TRANSFORMER PRIMARY VOLTAGE**

$$v'_{se} = L_m\frac{di_m}{dt}$$

EQUATION 4: **TRANSFORMER SECONDARY CURRENT**

$$abs(i_{sp}) = \left(1 + \frac{r_c}{R}\right)C_f\frac{dv_{cf}}{dt} + \frac{1}{R}\,v_{cf}$$

The output voltage (v_0) is shown in Equation 5.

EQUATION 5: **OUTPUT VOLTAGE**

$$v_o = r'_c \times abs(i_{sp}) + \left(\frac{r'_c}{r_c}\right)v_{cf}$$

Where:

$$r'_c = r_c \| R$$

AN1477

Applying Harmonic Approximation

The Fourier series decomposes periodic functions or periodic signals into a sum of (possibly infinite) simple oscillating functions (sines and cosines, or complex exponentials). Expressing the function ($f(x)$) as an infinite series of sine and cosine functions is shown in Equation 6.

EQUATION 6:   GENERAL FOURIER EXPANSION

$$f(x) = a_0 \pm \sum_{n=1}^{\infty} (a_n \sin(nx) + b_n \cos(nx))$$

$$= (a_0 \pm a_1 \sin(x) \pm a_2 \sin(2x) \pm a_3 \sin(3x) \pm b_1 \cos(x) \pm b_2 \cos(2x) \pm b_3 \cos(3x))$$

Expressing $f(x)$ by considering only the fundamental components and ignoring the DC component, and other harmonic terms is:

$$f(x) = a_1 \sin(x) \pm b_1 \cos(x)$$

The primary side resonant tank parameters, $i_r(t)$, $v_c(t)$ and $i_m(t)$, provided in Equation 7, are approximated to their fundamental harmonics, and the output filter voltage (v_{cf}) is approximated to the DC component. The derivatives of $i_r(t)$, $v_{cr}(t)$ and $i_m(t)$ are shown in Equation 7.

EQUATION 7:   FUNDAMENTAL APPROXIMATION OF PRIMARY TANK PARAMETERS

$$i_r(t) = i_s(t)\sin(\omega_s t) - i_c(t)\cos(\omega_s t)$$

$$v_{cr}(t) = v_s(t)\sin(\omega_s t) - v_c(t)\cos(\omega_s t)$$

$$i_m(t) = i_{ms}(t)\sin(\omega_s t) - i_{mc}(t)\cos(\omega_s t)$$

$$\frac{di_r}{dt} = \left(\frac{di_s}{dt} + \omega_s i_c\right)\sin(\omega_s t) - \left(\frac{di_c}{dt} - \omega_s i_s\right)\cos(\omega_s t)$$

$$\frac{dv_{cr}}{dt} = \left(\frac{dv_s}{dt} + \omega_s v_c\right)\sin(\omega_s t) - \left(\frac{dv_c}{dt} - \omega_s v_s\right)\cos(\omega_s t)$$

$$\frac{di_m}{dt} = \left(\frac{di_{ms}}{dt} + \omega_s i_{mc}\right)\sin(\omega_s t)$$

$$-\left(\frac{di_{mc}}{dt} - \omega_s i_{ms}\right)\cos(\omega_s t)$$

Where:

   ω_s = Switching frequency in radians/second
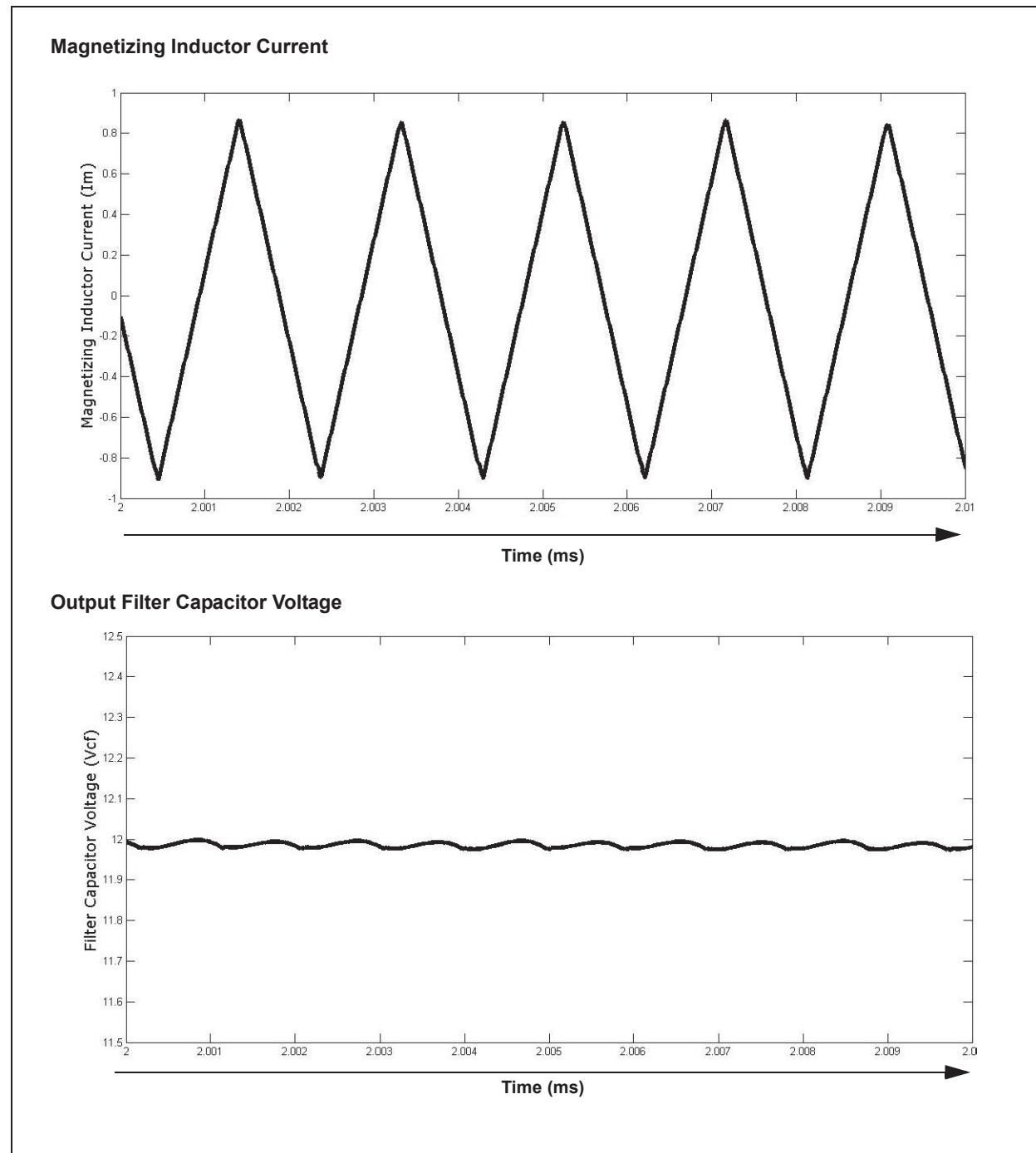
The amplitudes of sine component of resonant current (i_s), cosine component of resonant current (i_c), sine component of resonant capacitor voltage (v_s), cosine component of resonant capacitor voltage (v_c), sine component of magnetizing current (i_{ms}) and cosine component of magnetizing current (i_{mc}) are slow time varying components. Therefore, the dynamic behavior of these parameters can be analyzed.

Figure 3 and Figure 4 illustrate the simulation waveforms of the LLC resonant converter operating at below the resonant frequency and Continuous Tank Current mode.

FIGURE 3: SIMULATION WAVEFORMS OF LLC RESONANT CONVERTER

Input Voltage

Resonant Inductor Current

Resonant Capacitor Voltage
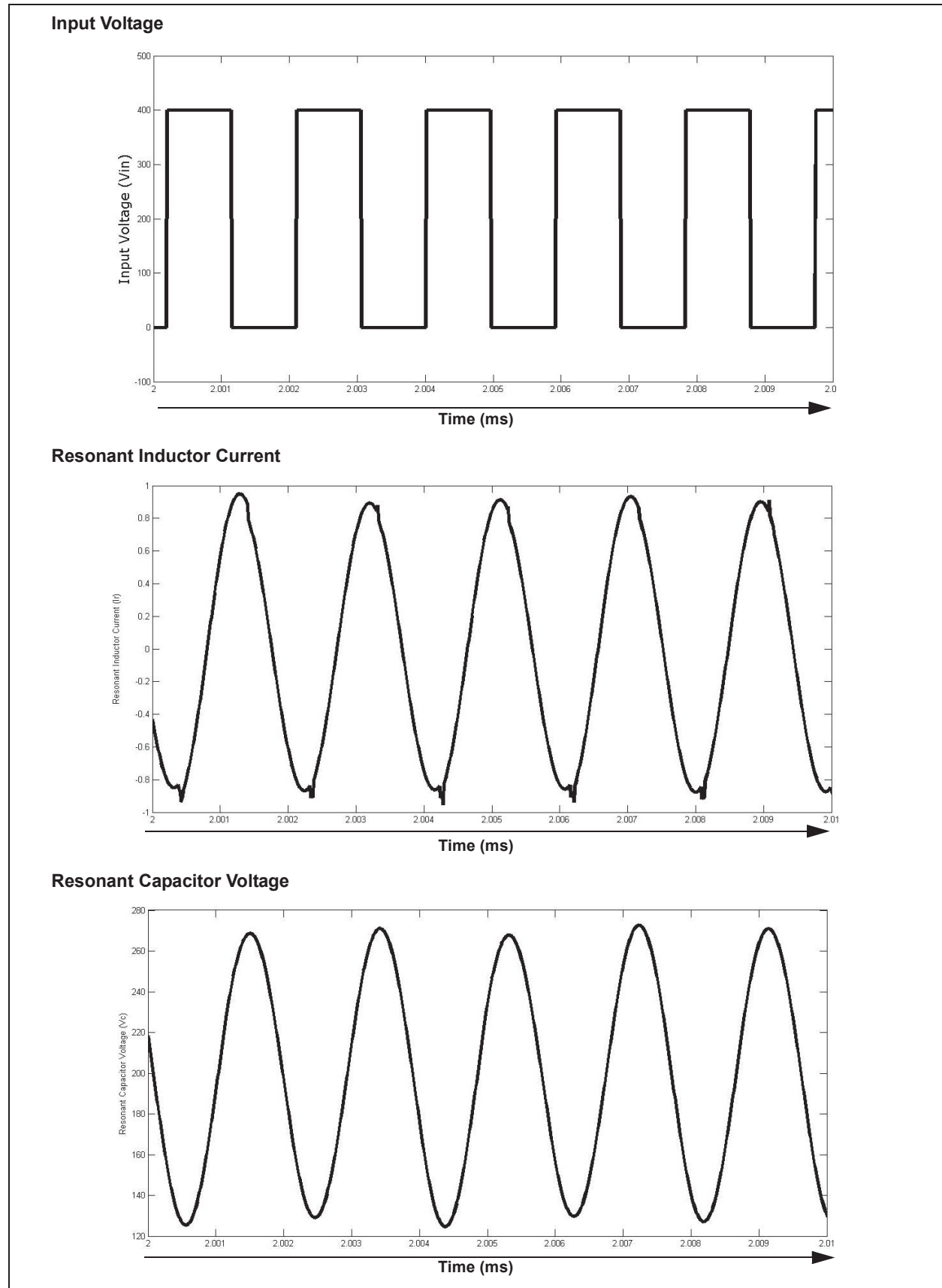
FIGURE 4: SIMULATION WAVEFORMS OF LLC RESONANT CONVERTER

Magnetizing Inductor Current

Output Filter Capacitor Voltage

Applying Extended Describing Function (EDF)

Extended Describing Function is a powerful mathematical approach for understanding, analyzing, improving and designing the behavior of nonlinear systems.

The nonlinear terms provided in Equation 1 through Equation 5, v_{se}' and $abs(i_{sp})$, can be approximated to their fundamental harmonic terms and DC terms.

The functions, $f_1(d, v_{in})$, $f_2(i_{ss}, i_{sp}, n \times abs(v_{se}))$, $f_3(i_{sc}, i_{sp}, n \times abs(v_{se}))$ and $f_4(i_{ss}, i_{sc})$, are called EDFs. Where i_{ss}, i_{sc} are the sine and cosine components of the transformer secondary current, and i_{sp} is the resultant current flowing in secondary. f_1, f_2, f_3 and f_4 are functions of the harmonic coefficients of state variables at chosen operating conditions. The EDF terms can be calculated by using the Fourier expansion of nonlinear terms. The EDF approximation to nonlinear states is shown in Equation 8.
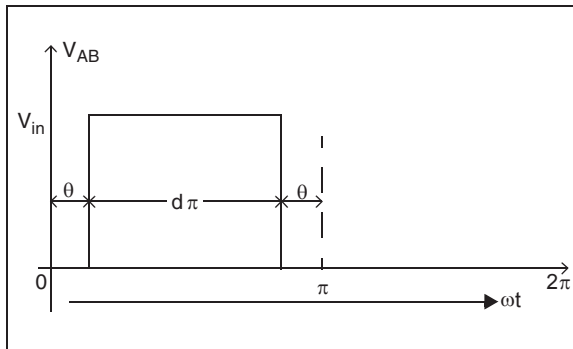
EQUATION 8:   EDF APPROXIMATION

$$v_{AB}(t) = f_1(d, v_{in})\sin(\omega_s t)$$

$$\operatorname{sgn}(i_{sp}) \times n \times abs(v_{se}) = f_2(i_{ss}, i_{sp}, n \times abs(v_{se}))\sin\omega_s t - f_3(i_{sc}, i_{sp}, n \times abs(v_{se}))$$

$$i_{sp} = f_4(i_{ss}, i_{sc})$$

Figure 5 illustrates a typical switching waveform of a half-bridge inverter which is the input to the LLC resonant tank (θ = Dead Time, d = Duty Cycle).

FIGURE 5:   OUTPUT SWITCHING WAVEFORM OF HALF-BRIDGE INVERTER

The fundamental output voltage of a half-bridge inverter is shown in Equation 9.

EQUATION 9:   OUTPUT VOLTAGE OF HALF-BRIDGE INVERTER

$$f_1(d, v_{in}) = \frac{2}{2\pi}\int_{\theta}^{(\pi-\theta)} v_{in} \times \sin(\omega t)d\omega t$$

$$f_1(d, v_{in}) = -\frac{2v_{in}}{2\pi}\cos(\omega t)\Big|_{\theta}^{(\pi-\theta)}$$

$$f_1(d, v_{in}) = \frac{2v_{in}}{2\pi}[\cos\theta - \cos(\pi-\theta)]$$

$$f_1(d, v_{in}) = \frac{2v_{in}}{\pi}\cos\theta = \frac{2v_{in}}{\pi}\times\cos\left(\frac{\pi}{2}-\frac{d\pi}{2}\right)$$

$$f_1(d, v_{in}) = \frac{2v_{in}}{\pi}\sin\left(\frac{\pi}{2}d\right) = v_{es}$$

Where:

$$\theta = \frac{\pi}{2} - \frac{d\pi}{2}$$

v_{es} = Sine component of the output voltage of half-bridge inverter

The switching waveform has an odd symmetry. Therefore, there is no cosine component ($v_{ec} = 0$, where v_{ec} is the cosine component of the output voltage of the half-bridge inverter) in the switching waveform and the sine component (v_{es}) forms the fundamental component of v_{AB}.

The second expression in Equation 8 is based on the fundamental frequency approximation. Fundamental component of transformer primary voltage can be decomposed in sine and cosine terms, where $f_2(i_{ss}, i_{sp}, n \times abs(v_{se}))$ and $f_3(i_{sc}, i_{sp}, n \times abs(v_{se}))$ are the magnitude of sine and cosine components, respectively. Derivation of f_2 and f_3 is shown in Equation 10. A factor of $4/\pi$ included in Equation 10 is based on the fundamental component of a square wave of transformer primary voltage.

The EDF approximation to the nonlinear transformer primary voltage is shown in Equation 10.

EQUATION 10: EDF APPROXIMATION TO TRANSFORMER PRIMARY VOLTAGE

$$f_2(i_{ss}, i_{sp}, n \times abs(v_{se})) = \frac{4}{\pi} \frac{i_{ss}}{i_{sp}} (n \times abs(v_{se}))$$

$$= \frac{4n}{\pi} \frac{i_{ps}}{i_{pp}} (abs(v_{se})) = v_{ps}$$

$$f_3(i_{sc}, i_{sp}, n \times abs(v_{se})) = \frac{4}{\pi} \frac{i_{sc}}{i_{sp}} (n \times abs(v_{se}))$$

$$= \frac{4n}{\pi} \frac{i_{pc}}{i_{pp}} (abs(v_{se})) = v_{pc}$$

$$i_{pp} = \sqrt{i_{ps}^2 + i_{pc}^2}$$

Where:

v_{ps}, v_{pc}	= Sine, cosine components of the transformer primary voltage
i_{ps}, i_{pc}	= Sine, cosine components of the transformer primary current
i_{pp}	= Resultant transformer primary current
i_{ss}, i_{sc}	= Sine, cosine components of the transformer secondary current
i_{sp}	= Resultant current flowing in secondary
$n = np/ns$	= Transformer turns ratio

Harmonic Balance

Harmonic balance is a frequency domain method used to calculate the steady-state response of nonlinear differential equations. The term, "harmonic balance", is descriptive of the method, which uses the Kirchhoff's Current Laws (KCLs) written in the frequency domain and a chosen number of harmonics. Effectively, the method assumes that the solution can be represented by a linear combination of sinusoids, and then balances current and voltage sinusoids to satisfy the Kirchhoff's Laws. The harmonic balance method is commonly used to simulate circuits which include nonlinear elements.

Substituting Equation 9 and Equation 10 into Equation 1 through Equation 5, and separating the DC, sine and cosine terms, Equation 11 through Equation 13 are obtained.

EQUATION 11: SINE AND COSINE COMPONENTS OF TANK VOLTAGE

$$v_{es} = L_s\left(\frac{di_s}{dt} + \omega_s i_c\right) + r_s i_s + v_s + v_{ps}$$

$$= L_s\left(\frac{di_s}{dt} + \omega_s i_c\right) + r_s i_s + v_s + \frac{4n}{\pi}\frac{i_{ps}}{i_{pp}} abs(v_{se})$$

$$v_{ec} = L_s\left(\frac{di_c}{dt} - \omega_s i_s\right) + r_s i_c + v_c + v_{pc}$$

$$= L_s\left(\frac{di_c}{dt} - \omega_s i_s\right) + r_s i_c + v_c + \frac{4n}{\pi}\frac{i_{pc}}{i_{pp}} abs(v_{se})$$

EQUATION 12: SINE AND COSINE COMPONENTS OF TANK CURRENT

$$i_s = C_s\left(\frac{dv_s}{dt} + \omega_s v_c\right)$$

$$i_c = C_s\left(\frac{dv_c}{dt} - \omega_s v_s\right)$$

EQUATION 13: SINE AND COSINE COMPONENT OF TRANSFORMER PRIMARY VOLTAGE

$$L_m\left(\frac{di_{ms}}{dt} + \omega_s i_{mc}\right) = \frac{4n}{\pi}\frac{i_{ps}}{i_{pp}} abs(v_{se}) = v_{ps}$$

$$L_m\left(\frac{di_{mc}}{dt} - \omega_s i_{ms}\right) = \frac{4n}{\pi}\frac{i_{pc}}{i_{pp}} abs(v_{se}) = v_{pc}$$

Only the DC term is considered for the output capacitor voltage, as shown in Equation 14.

EQUATION 14: OUTPUT FILTER CAPACITOR VOLTAGE

$$\left(1 + \frac{r_c}{R}\right) C_f \frac{dv_{c_f}}{dt} + \frac{1}{R} v_{c_f} = \frac{2}{\pi} i_{sp}$$

The output voltage equation is shown in Equation 15.

EQUATION 15: OUTPUT VOLTAGE

$$v_0 = \frac{2}{\pi} r'_c\, i_{sp} + \left(\frac{r'_c}{r_c}\right) v_{c_f}$$

Equation 11 through Equation 15 are the nonlinear large signal model of the LLC resonant converter power stage and are illustrated in Figure 6. It is important to note that the input of Equation 12 through Equation 15, $\{v_g, \omega_s, d\}$, is slow varying quantities with respect to the switching frequency. Therefore, the modulation equations can be easily perturbed and linearized at chosen operating points.

FIGURE 6: LARGE SIGNAL MODEL OF LLC RESONANT CONVERTER
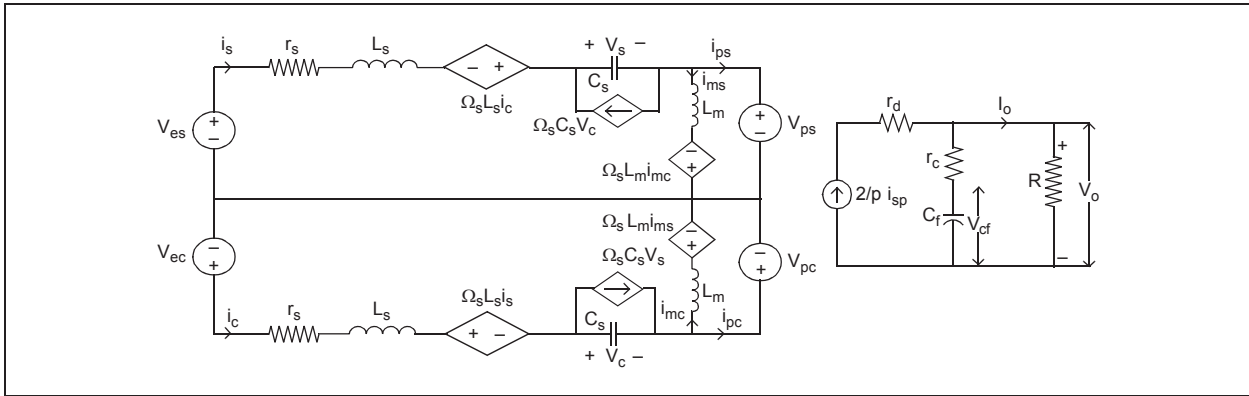
Deriving Steady-State Operating Point

Under steady-state conditions, the state variables of the modulation equations, Equation 12 through Equation 14, do not change with time. For a chosen operating point, the time derivatives in Equation 12 through Equation 14 are set to zero and the steady-state values are obtained (shown in upper case letters). The transformer currents on the primary and secondary sides are shown in Equation 16.

EQUATION 16: TRANSFORMER CURRENTS

Primary Current:
$$i_{pp} = \sqrt{i_{ps}^2 + i_{pc}^2}$$

Secondary Current:
$$i_{sp} = \sqrt{i_{ss}^2 + i_{sc}^2} = n\sqrt{i_{ps}^2 + i_{pc}^2} = n i_{pp}$$

Where:
$n = np/ns$ = Transformer turns ratio

The output filter capacitor voltage in steady-state conditions can be calculated by substituting Equation 16 into Equation 14, as shown in Equation 17.

EQUATION 17: FILTER CAPACITOR VOLTAGE

$$\frac{V_{c_f}}{R} = \frac{2n}{\pi} I_{pp} = \frac{2}{\pi} I_{sp}$$

$$\Rightarrow V_{c_f} = \frac{2n}{\pi} I_{pp} R$$

Transformer secondary voltage in steady-state is derived using Equation 15, which is shown in Equation 18. The steady-state analysis for the tank current, resonant capacitor voltage and magnetizing current are provided in Equation 19 through Equation 23.

AN1477

EQUATION 18: TRANSFORMER SECONDARY VOLTAGE

$$abs(v_{se}) = r_d \frac{2}{\pi} i_{sp} + v_o$$

$$= r_d \frac{2}{\pi} I_{sp} + \frac{2}{\pi} r_c{'} I_{sp} + \left(\frac{r_c{'}}{r_c}\right) V_{c_f}$$

$$= (r_d + r_c{'}) \frac{2n}{\pi} I_{pp} + \left(\frac{r_c{'}}{r_c}\right) \frac{2n}{\pi} I_{pp} R$$

$$= \left[(r_d + r_c{'}) + \left(\frac{r_c{'}}{r_c}\right) R\right] \frac{2n}{\pi} I_{pp}$$

$$= (r_d + R) \frac{2n}{\pi} I_{pp}$$

Substituting the value of Equation 17 into the sine component of tank voltage, the result obtained is shown in Equation 19.

EQUATION 19: SINE COMPONENT OF TANK VOLTAGE

$$v_{es} = L_s\left(\frac{di_s}{dt} + \omega_s i_c\right) + r_s i_s + v_s + \frac{4}{\pi} \frac{i_{ps}}{i_{pp}} n \times abs(v_{se})$$

$$\Rightarrow L_s \Omega_s I_c + r_s I_s + V_s + \frac{4}{\pi} \frac{I_{ps}}{I_{pp}} \frac{2n^2}{\pi} (r_d + R) I_{pp}$$
$$= V_{es} = \frac{2}{\pi} V_{in}$$

$$\Rightarrow r_s I_s + L_s \Omega_s I_c + V_s + R_e I_{ps} = \frac{2}{\pi} V_{in}$$

$$\Rightarrow (r_s + R_e) I_s + L_s \Omega_s I_c + V_s - R_e I_{ms} = \frac{2}{\pi} V_{in}$$

Where:
$$I_{ps} = I_s - I_{ms}$$
$$R_e = \frac{8n^2}{\pi^2} [r_d + R]$$

Substituting the value of Equation 17 into the cosine component of the tank voltage, the result obtained is shown in Equation 20.

EQUATION 20: COSINE COMPONENT OF TANK VOLTAGE

$$v_{ec} = L_s\left(\frac{di_c}{dt} - \omega_s i_s\right) + r_s i_c + v_c + \frac{4}{\pi} \frac{i_{pc}}{i_{pp}} n \times abs(v_{se})$$

$$\Rightarrow -L_s \Omega_s I_s + r_s I_c + V_c + \frac{4}{\pi} \frac{I_{pc}}{I_{pp}} \frac{2n^2}{\pi} (r_d + R) I_{pp}$$
$$= V_{ec} = 0$$

$$\Rightarrow -L_s \Omega_s I_s + r_s I_c + V_c + I_{pc} R_e = 0$$

$$\Rightarrow -L_s \Omega_s I_s + (r_s + R_e) I_c + V_c - I_{mc} R_e = 0$$

Where:
$$I_{pc} = I_c - I_{mc}$$

The steady-state values of sine and cosine components of the tank current can be obtained by equating dv_s/dt and dv_c/dt to zero. The result is shown in Equation 21.

EQUATION 21: SINE AND COSINE COMPONENTS OF TANK CURRENT

$$C_s\left(\frac{dv_s}{dt} + \omega_s v_c\right) = i_s$$
$$\Rightarrow I_s - C_s \Omega_s V_c = 0$$
$$C_s\left(\frac{dv_c}{dt} - \omega_s v_s\right) = i_c$$
$$I_c + C_s \Omega_s V_s = 0$$

Substituting the value of Equation 17 into the sine component of magnetizing current, the result is shown in Equation 22.

EQUATION 22: SINE COMPONENT OF MAGNETIZING CURRENT

$$L_m\left(\frac{di_{ms}}{dt} + \omega_s i_{mc}\right) = \frac{4}{\pi} \times \frac{i_{ps}}{i_{pp}} \times n \times abs(v_{se})$$

$$\Rightarrow L_m \Omega_s I_{mc} - R_e I_{ps} = 0$$

$$\Rightarrow R_e I_s - L_m \Omega_s I_{mc} - R_e I_{ms} = 0$$

Substituting the value of Equation 17 into the cosine component of magnetizing current, the result is shown in Equation 23.

EQUATION 23: COSINE COMPONENT OF MAGNETIZING CURRENT

$$L_m\left(\frac{di_{mc}}{dt} - \omega_s i_{ms}\right) = \frac{4n}{\pi}\frac{i_{pc}}{i_{pp}}n \times abs(v_{se})$$

$$\Rightarrow (-L_m\Omega_s I_{ms}) - R_e I_{pc} = 0$$

$$\Rightarrow L_m\Omega_s I_{ms} + R_e I_c - R_e I_{mc} = 0$$

Equation 20 through Equation 23 are arranged, as shown in Equation 24.

EQUATION 24: ARRANGEMENT OF STEADY-STATE EQUATIONS

$$(r_s + R_e)I_s + L_s\Omega_s I_c + V_s - R_e I_{ms} = \frac{2}{\pi}V_{in} = V_{es}$$

$$-L_s\Omega_s I_s + (r_s + R_e)I_c + V_c - I_{mc}R_e = 0 = V_{ec}$$

$$I_s - C_s\Omega_s V_c = 0$$

$$I_c + C_s\Omega_s V_s = 0$$

$$R_e I_s - L_m\Omega_s I_{mc} - R_e I_{ms} = 0$$

$$L_m\Omega_s I_{ms} + R_e I_c - R_e I_{mc} = 0$$

To obtain the tank current, capacitor voltage and magnetizing current from the steady-state equations, Equation 24 is formulated in the matrix form, as shown in Equation 25.

EQUATION 25: STEADY-STATE OPERATING POINT

$$X \times Y = U_0$$

$$Y = X^{-1} \times U_0$$

Where:

$$X = \begin{bmatrix} r_s + R_e & L_s\Omega_s & 1 & 0 & -R_e & 0 \\ -L_s\Omega_s & r_s + R_e & 0 & 1 & 0 & -R_e \\ 1 & 0 & 0 & -C_s\Omega_s & 0 & 0 \\ 0 & 1 & C_s\Omega_s & 0 & 0 & 0 \\ R_e & 0 & 0 & 0 & -R_e & -L_m\Omega_s \\ 0 & R_e & 0 & 0 & L_m\Omega_s & -R_e \end{bmatrix}$$

$$U_0 = \begin{bmatrix} V_{es} \\ 0 \\ 0 \\ 0 \\ 0 \\ 0 \end{bmatrix} \qquad Y = \begin{bmatrix} I_s \\ I_c \\ V_s \\ V_c \\ I_{ms} \\ I_{mc} \end{bmatrix}$$

Perturbation and Linearization of Harmonic Balance Equations

The nonlinear system equations, Equation 12 through Equation 14, are in the form of: $x' = f(x(t), u(t))$; $x(t)$ = state of the nonlinear system and $u(t)$ = input to the system.

The function (x') can be linearized about an operating point and is expressed in the form of: $x' = Ax + Bu$, where A and B are the Jacobian matrices of the system with respect to $x(t)$ and $u(t)$, as shown in Equation 26.

EQUATION 26: JACOBIAN MATRICES

$$A_{ij} = \frac{\delta f(x(t),u(t))_i}{\partial x_j(t)}\bigg|_{x_0,\,u_0}$$

$$B_{ij} = \frac{\delta f(x(t),u(t))_i}{\partial u_j(t)}\bigg|_{x_0,\,u_0}$$

Where:

x_0 and u_0 represent the steady-state operating points.

In the perturbation and linearization step, it is assumed that the averaged state variables and the input variables consist of the constant DC component, and a small signal AC variation about the DC component. Perturbed signals are shown in Equation 27.

EQUATION 27: PERTURBED SIGNALS

$$v_{in} = V_{in} + \hat{v}_{in}, \quad d = D + \hat{d}, \quad \omega_s = \Omega_s + \hat{\omega}_s, \quad v_{ps} = V_{ps} + \hat{v}_{ps}, \quad v_{pc} = V_{pc} + \hat{v}_{pc}, \quad i_{ps} = I_{ps} + \hat{i}_{ps},$$

$$i_{pc} = I_{pc} + \hat{i}_{pc}, \quad i_{pp} = I_{pp} + \hat{i}_{pp}, \quad v_{c_f} = V_{c_f} + \hat{v}_{c_f}, \quad i_{ms} = I_{ms} + \hat{i}_{ms}, \quad i_{mc} = I_{mc} + \hat{i}_{mc}, \quad i_s = I_s + \hat{i}_s,$$

$$i_c = I_c + \hat{i}_c, \quad v_s = V_s + \hat{v}_s, \quad v_c = V_c + \hat{v}_c, \quad v_{es} = V_{es} + \hat{v}_{es}, \quad v_0 = V_0 + \hat{v}_0$$

The sine component of the transformer primary voltage (v_{ps}) is linearized around the steady-state operating point, as shown in Equation 28.

EQUATION 28: LINEARIZATION OF SINE COMPONENT OF TRANSFORMER PRIMARY VOLTAGE

$$v_{ps} = \frac{4n}{\pi}\frac{i_{ps}}{i_{pp}}abs(v_{se}) = \frac{4n}{\pi}\left(\frac{r'_c}{r_c}\right)\frac{i_{ps}}{\sqrt{i_{ps}^2 + i_{pc}^2}}v_{cf} + \frac{8n^2}{\pi^2}(r_d + r'_c)i_{ps}$$

$$\hat{v}_{ps} = \frac{4nV_{cf}}{\pi}\left(\frac{r'_c}{r_c}\right)\left(\frac{\sqrt{I_{ps}^2 + I_{pc}^2} - \frac{I_{ps}^2}{\sqrt{I_{ps}^2 + I_{pc}^2}}}{I_{ps}^2 + I_{pc}^2}\right)\hat{i}_{ps} - \frac{4nV_{cf}}{\pi}\left(\frac{r'_c}{r_c}\right)\left(\frac{I_{ps}I_{pc}}{\left(I_{ps}^2 + I_{pc}^2\right)^{\frac{3}{2}}}\right)\hat{i}_{pc}$$

$$+ \frac{4n}{\pi}\left(\frac{r'_c}{r_c}\right)\left(\frac{I_{ps}}{\sqrt{I_{ps}^2 + I_{pc}^2}}\right)\hat{v}_{cf} + \frac{8n^2}{\pi^2}(r_d + r'_c)\hat{i}_{ps}$$

$$\hat{v}_{ps} = \left(\frac{r'_c}{r_c}\right)\left(\frac{4nV_{cf}}{\pi}\frac{I_{pc}^2}{I_{pp}^3}\hat{i}_{ps} - \frac{4nV_{cf}}{\pi}\frac{I_{ps}I_{pc}}{I_{pp}^3}\hat{i}_{pc} + \frac{4n}{\pi}\frac{I_{ps}}{I_{pp}}\hat{v}_{cf}\right) + \frac{8n^2}{\pi^2}(r_d + r'_c)\hat{i}_{ps}$$

$$H_{ip} = \frac{4nV_{cf}}{\pi}\left(\frac{r'_c}{r_c}\right)\frac{I_{pc}^2}{I_{pp}^3} + \frac{8n^2}{\pi^2}(r_d + r'_c)$$

$$H_{ic} = -\frac{4nV_{cf}}{\pi}\left(\frac{r'_c}{r_c}\right)\frac{I_{ps}I_{pc}}{I_{pp}^3}$$

$$H_{vcf} = \frac{4n}{\pi}\left(\frac{r'_c}{r_c}\right)\frac{I_{ps}}{I_{pp}}$$

The cosine component of the transformer primary voltage (v_{pc}) is linearized around the steady-state operating point, as shown in Equation 29.

EQUATION 29:   LINEARIZATION OF COSINE COMPONENT OF TRANSFORMER PRIMARY VOLTAGE

$$v_{pc} = \frac{4n}{\pi} \frac{i_{pc}}{i_{pp}} abs(v_{se}) = \frac{4n}{\pi}\left(\frac{r'_c}{r_c}\right) \frac{i_{pc}}{\sqrt{i_{ps}^2 + i_{pc}^2}} v_{cf} + \frac{8n^2}{\pi^2}(r_d + r'_c)i_{pc}$$

$$\hat{v}_{pc} = -\frac{4nV_{cf}}{\pi}\left(\frac{r'_c}{r_c}\right)\left(\frac{I_{ps} I_{pc}}{(I_{ps}^2 + I_{pc}^2)^{\frac{3}{2}}}\right)\hat{i}_{ps} + \frac{4nV_{cf}}{\pi}\left(\frac{r'_c}{r_c}\right)\left(\frac{\sqrt{I_{ps}^2 + I_{pc}^2} - \frac{I_{pc}^2}{\sqrt{I_{ps}^2 + I_{pc}^2}}}{I_{ps}^2 + I_{pc}^2}\right)\hat{i}_{pc}$$

$$+ \frac{4n}{\pi}\left(\frac{r'_c}{r_c}\right)\left(\frac{I_{pc}}{\sqrt{I_{ps}^2 + I_{pc}^2}}\right)\hat{v}_{cf} + \frac{8n^2}{\pi^2}(r_d + r'_c)\hat{i}_{pc}$$

$$\hat{v}_{ps} = \left(\frac{r'_c}{r_c}\right)\left(-\frac{4nV_{cf}}{\pi} \frac{I_{ps} I_{pc}}{I_{pp}^3}\hat{i}_{ps} + \frac{4nV_{cf}}{\pi} \frac{I_{ps}^2}{I_{pp}^3}\hat{i}_{pc} + \frac{4n}{\pi} \frac{I_{pc}}{I_{pp}}\hat{v}_{cf}\right) + \frac{8n^2}{\pi^2}(r_d + r'_c)\hat{i}_{pc}$$

$$G_{ip} = -\frac{4nV_{cf}}{\pi}\left(\frac{r'_c}{r_c}\right)\frac{I_{ps} I_{pc}}{I_{pp}^3}$$

$$G_{ic} = \frac{4nV_{cf}}{\pi}\left(\frac{r'_c}{r_c}\right)\frac{I_{ps}^2}{I_{pp}^3} + \frac{8n^2}{\pi^2}(r_d + r'_c)$$

$$G_{vcf} = \frac{4n}{\pi}\left(\frac{r'_c}{r_c}\right)\frac{I_{pc}}{I_{pp}}$$

The linearization of the input voltage (v_{es}) is shown in Equation 30.

EQUATION 30: LINEARIZATION OF HALF-BRIDGE INVERTER OUTPUT VOLTAGE

$$v_{es} = \frac{2v_{in}}{\pi} \sin\left(\frac{\pi}{2}d\right)$$

$$V_{es} + \hat{v}_{es} = \frac{2}{\pi} \times (V_{in} + \hat{v}_{in})\sin\left(\frac{\pi}{2}(D + \hat{d})\right)$$

Expanding $\sin\left(\frac{\pi}{2}(D + \hat{d})\right)$

$$= \sin\left(\frac{\pi}{2}D\right)\cos\left(\frac{\pi}{2}\hat{d}\right) + \cos\left(\frac{\pi}{2}D\right)\sin\left(\frac{\pi}{2}\hat{d}\right)$$

$$= \sin\left(\frac{\pi}{2}D\right) + \frac{\pi}{2}\cos\left(\frac{\pi}{2}D\right)\hat{d}$$

$$V_{es} + \hat{v}_{es} = \frac{2}{\pi}(V_{in} + \hat{v}_{in})\left(\sin\left(\frac{\pi}{2}D\right) + \frac{\pi}{2}\cos\left(\frac{\pi}{2}D\right)\hat{d}\right)$$

Removing the steady-state terms and other higher order perturbed terms in Equation 30 to get the linearized input voltage, as shown in Equation 31.

EQUATION 31: LINEARIZATION OF HALF-BRIDGE INVERTER OUTPUT VOLTAGE

$$\hat{v}_{es} = \frac{2}{\pi}\sin\left(\frac{\pi}{2}D\right)\hat{v}_{in} + V_{in}\cos\left(\frac{\pi}{2}D\right)\hat{d}$$

$$\hat{v}_{es} = K_1\hat{v}_{in} + K_2\hat{d}$$

Where:

$$K_1 = \frac{2}{\pi}\sin\left(\frac{\pi}{2}D\right)$$

$$K_2 = V_{in}\cos\left(\frac{\pi}{2}D\right)$$

The linearization and perturbation of the tank current, capacitor voltage, transformer primary voltage, output voltage and output filter capacitor voltage, after removing the second order and DC terms, are provided in Equation 32 through Equation 43.

In resonant converters, the poles and zeroes are the functions of normalized switching frequency ($\omega_{sn} = \omega_s/\omega_0$), where ω_s is the switching frequency and ω_0 is the resonant frequency.

The linearization and perturbation of the sine component of the tank voltage is provided in Equation 32.

EQUATION 32: LINEARIZATION OF SINE COMPONENT OF TANK VOLTAGE

$$L_s\frac{d(I_s + \hat{i}_s)}{dt} + r_s(I_s + \hat{i}_s) + L_s(I_c + \hat{i}_c)\left(\Omega_s + \omega_0\frac{\hat{\omega}_s}{\omega_0}\right) + (V_s + \hat{v}_s) + (V_{ps} + \hat{v}_{ps}) = (V_{es} + \hat{v}_{es})$$

$$L_s\frac{d\hat{i}_s}{dt} + r_s\hat{i}_s + \Omega_s L_s\hat{i}_c + L_s\omega_0 I_c\hat{\omega}_{sn} + \hat{v}_s + \hat{v}_{ps} = \hat{v}_{es}$$

Substitute the values of Equation 28 and Equation 31 into the sine component of the tank voltage, as shown in Equation 33.

EQUATION 33: LINEARIZATION OF SINE COMPONENT OF TANK VOLTAGE

$$L_s\frac{d\hat{i}_s}{dt} + r_s\hat{i}_s + \Omega_sL_s\hat{i}_c + L_s\omega_0 I_c\hat{\omega}_{sn} + \hat{v}_s + H_{ip}\hat{i}_s + H_{ic}\hat{i}_c - H_{ip}\hat{i}_{ms} - H_{ic}\hat{i}_{mc} + H_{vcf}\hat{V}c_f = K_1\hat{v}_{in} + K_2\hat{d}$$

$$L_s\frac{d\hat{i}_s}{dt} = -(H_{ip}+r_s)\hat{i}_s - (\Omega_sL_s+H_{ic})\hat{i}_c - \hat{v}_s + H_{ip}\hat{i}_{ms} + H_{ic}\hat{i}_{mc} - H_{vcf}\hat{V}c_f + K_1\hat{v}_{in} + K_2\hat{d} - L_s\omega_0 I_c\hat{\omega}_{sn}$$

$$\frac{d\hat{i}_s}{dt} = -\left(\frac{H_{ip}+r_s}{L_s}\right)\hat{i}_s - \left(\frac{\Omega_sL_s+H_{ic}}{L_s}\right)\hat{i}_c - \frac{1}{L_s}\hat{v}_s + \frac{H_{ip}}{L_s}\hat{i}_{ms} + \frac{H_{ic}}{L_s}\hat{i}_{mc} - \frac{H_{vcf}}{L_s}\hat{V}c_f + \frac{K_1}{L_s}\hat{v}_{in} + \frac{K_2}{L_s}\hat{d} - \frac{L_s\omega_0 I_c}{L_s}\hat{\omega}_{sn}$$

The linearization and perturbation of the cosine component of tank voltage is provided in Equation 34.

EQUATION 34: LINEARIZATION OF COSINE COMPONENT OF TANK VOLTAGE

$$L_s\frac{d(I_c+\hat{i}_c)}{dt} + r_s(I_c+\hat{i}_c) - L_s(I_s+\hat{i}_s)\left(\Omega_s + \omega_0\frac{\hat{\omega}_s}{\omega_0}\right) + (V_c+\hat{v}_c) + (V_{pc}+\hat{v}_{pc}) = 0$$

$$\left(L_s\frac{d\hat{i}_c}{dt} + r_s\hat{i}_c\right) - \Omega_sL_s\hat{i}_s - L_s\omega_0 I_s\hat{\omega}_{sn} + \hat{v}_c + \hat{v}_{pc} = 0$$

Substituting the values of Equation 29 into the cosine component of the tank voltage, the result obtained is shown in Equation 35.

EQUATION 35: LINEARIZATION OF COSINE COMPONENT OF TANK VOLTAGE

$$\left(L_s\frac{d\hat{i}_c}{dt} + r_s\hat{i}_c\right) - \Omega_sL_s\hat{i}_s - L_s\omega_0 I_s\hat{\omega}_{sn} + \hat{v}_c + G_{ip}\hat{i}_s + G_{ic}\hat{i}_c - G_{ip}\hat{i}_{ms} - G_{ic}\hat{i}_{mc} + G_{vcf}\hat{v}c_f = 0$$

$$L_s\frac{d\hat{i}_c}{dt} = (\Omega_sL_s - G_{ip})\hat{i}_s - (G_{ic}+r_s)\hat{i}_c - \hat{v}_c + G_{ip}\hat{i}_{ms} + G_{ic}\hat{i}_{mc} - G_{vcf}\hat{v}c_f + L_s\omega_0 I_s\hat{\omega}_{sn}$$

$$\frac{d\hat{i}_c}{dt} = \frac{(\Omega_sL_s - G_{ip})}{L_s}\hat{i}_s - \frac{(G_{ic}+r_s)}{L_s}\hat{i}_c - \frac{1}{L_s}\hat{v}_c + \frac{G_{ip}}{L_s}\hat{i}_{ms} + \frac{G_{ic}}{L_s}\hat{i}_{mc} - \frac{G_{vcf}}{L_s}\hat{v}c_f + \frac{L_s\omega_0 I_s}{L_s}\hat{\omega}_{sn}$$

The linearization and perturbation of the sine component of the tank current is provided in Equation 36.

EQUATION 36: LINEARIZATION OF SINE COMPONENT OF TANK CURRENT

$$C_s\frac{d(V_s+\hat{v}_s)}{dt} + C_s(V_c+\hat{v}_c)\left(\Omega_s + \omega_0\frac{\hat{\omega}_s}{\omega_0}\right) = (I_s+\hat{i}_s)$$

$$C_s\frac{d\hat{v}_s}{dt} + C_s\Omega_s\hat{v}_c + C_s\omega_0 V_c\hat{\omega}_{sn} = \hat{i}_s$$

$$\frac{d\hat{v}_s}{dt} = \frac{1}{C_s}\hat{i}_s - \frac{C_s\Omega_s}{C_s}\hat{v}_c - \frac{C_s\omega_0 V_c}{C_s}\hat{\omega}_{sn}$$

The linearization and perturbation of the cosine component of the tank current is provided in Equation 37.

EQUATION 37: LINEARIZATION OF COSINE COMPONENT OF TANK CURRENT

$$C_s\frac{d(V_c+\hat{v}_c)}{dt} - C_s(V_s+\hat{v}_s)\left(\Omega_s + \omega_0\frac{\hat{\omega}_s}{\omega_0}\right) = (I_c+\hat{i}_c)$$

$$\left(C_s\frac{d\hat{v}_c}{dt} - C_s\Omega_s\hat{v}_s\right) - C_s\omega_0 V_c\hat{\omega}_{sn} = \hat{i}_c$$

$$\frac{d\hat{v}_c}{dt} = \frac{1}{C_s}\hat{i}_c + \frac{C_s\Omega_s}{C_s}\hat{v}_s + \frac{C_s\omega_0 V_s}{C_s}\hat{\omega}_{sn}$$

AN1477

The linearization and perturbation of the sine component of the magnetizing current is provided in Equation 38.

EQUATION 38: LINEARIZATION OF SINE COMPONENT OF MAGNETIZING CURRENT

$$L_m \frac{d(I_{ms} + \hat{i}_{ms})}{dt} + L_m(I_{mc} + \hat{i}_{mc})\left(\Omega_s + \omega_0 \frac{\hat{\omega}_s}{\omega_0}\right) = (V_{ps} + \hat{v}_{ps})$$

$$L_m \frac{d\hat{i}_{ms}}{dt} + L_m \Omega_s \hat{i}_{mc} + L_m I_{mc} \omega_0 \hat{\omega}_{sn} = \hat{v}_{ps}$$

Substituting the value of Equation 28 into the sine component of the transformer primary voltage, the results are shown in Equation 39.

EQUATION 39: LINEARIZATION OF SINE COMPONENT OF MAGNETIZING CURRENT

$$L_m \frac{d\hat{i}_{ms}}{dt} + L_m \Omega_s \hat{i}_{mc} + L_m I_{mc} \omega_0 \hat{\omega}_{sn} = H_{ip}\hat{i}_s + H_{ic}\hat{i}_c - H_{ip}\hat{i}_{ms} - H_{ic}\hat{i}_{mc} + H_{vcf}\hat{v}_{cf}$$

$$L_m \frac{d\hat{i}_{ms}}{dt} = H_{ip}\hat{i}_s + H_{ic}\hat{i}_c - H_{ip}\hat{i}_{ms} - (H_{ic} + L_m \Omega_s)\hat{i}_{mc} + H_{vcf}\hat{v}_{cf} - L_m I_{mc} \omega_0 \hat{\omega}_{sn}$$

$$\frac{d\hat{i}_{ms}}{dt} = \frac{H_{ip}}{L_m}\hat{i}_s + \frac{H_{ic}}{L_m}\hat{i}_c - \frac{H_{ip}}{L_m}\hat{i}_{ms} - \frac{(H_{ic} + L_m \Omega_s)}{L_m}\hat{i}_{mc} + \frac{H_{vcf}}{L_m}\hat{v}_{cf} - \frac{L_m I_{mc} \omega_0}{L_m}\hat{\omega}_{sn}$$

The linearization and perturbation of the cosine component of the tank voltage is provided in Equation 40.

EQUATION 40: LINEARIZATION OF COSINE COMPONENT OF MAGNETIZING CURRENT

$$L_m \frac{d(I_{mc} + \hat{i}_{mc})}{dt} - L_m(I_{ms} + \hat{i}_{ms})\left(\Omega_s + \omega_0 \frac{\hat{\omega}_s}{\omega_0}\right) = (V_{pc} + \hat{v}_{pc})$$

$$L_m \frac{d\hat{i}_{mc}}{dt} - L_m \Omega_s \hat{i}_{ms} - L_m I_{ms} \omega_0 \hat{\omega}_{sn} = \hat{v}_{pc}$$

Substituting Equation 29 into the cosine component of the magnetizing current, the result is shown in Equation 41.

EQUATION 41: LINEARIZATION OF COSINE COMPONENT OF MAGNETIZING CURRENT

$$L_m \frac{d\hat{i}_{mc}}{dt} - L_m \Omega_s \hat{i}_{ms} - L_m I_{ms} \omega_0 \hat{\omega}_{sn} = G_{ip}\hat{i}_s + G_{ic}\hat{i}_c - G_{ip}\hat{i}_{ms} - G_{ic}\hat{i}_{mc} + G_{vcf}\hat{v}_{cf}$$

$$\frac{d\hat{i}_{mc}}{dt} = \frac{G_{ip}}{L_m}\hat{i}_s + \frac{G_{ic}}{L_m}\hat{i}_c - \frac{(G_{ip} - L_m \Omega_s)}{L_m}\hat{i}_{ms} - \frac{G_{ic}}{L_m}\hat{i}_{mc} + \frac{G_{vcf}}{L_m}\hat{v}_{cf} + \frac{L_m I_{ms} \omega_0}{L_m}\hat{\omega}_{sn}$$

The linearization and perturbation of the output filter capacitor voltage is provided in Equation 42.

EQUATION 42:   LINEARIZATION OF OUTPUT CAPACITOR VOLTAGE

$$\left(1 + \frac{r_c}{R}\right)C_f \frac{d\left(V_{c_f} + \hat{v}_{c_f}\right)}{dt} + \frac{1}{R}\left(V_{c_f} + \hat{v}_{c_f}\right) = \frac{2}{\pi}(I_{sp} + \hat{i}_{sp})$$

$$\Rightarrow \left(1 + \frac{r_c}{R}\right)C_f \times \frac{d\hat{v}_{c_f}}{dt} + \frac{1}{R}\hat{v}_{c_f} = \frac{2}{\pi}\hat{i}_{sp}$$

From Equation 16:

$$\frac{2}{\pi}i_{sp} = \frac{2n}{\pi}\sqrt{i_{ps}^2 + i_{pc}^2}$$

$$\frac{2}{\pi}\hat{i}_{sp} = \frac{2n}{\pi}\frac{I_{ps}}{\sqrt{I_{ps}^2 + I_{pc}^2}}\hat{i}_{ps} + \frac{2n}{\pi}\frac{I_{pc}}{\sqrt{I_{ps}^2 + I_{pc}^2}}\hat{i}_{pc}$$

$$\Rightarrow K_{is}\hat{i}_{ps} + K_{ic}\hat{i}_{pc}$$

$$\frac{2}{\pi}\hat{i}_{sp} = K_{is}\hat{i}_s + K_{ic}\hat{i}_c - K_{is}\hat{i}_{ms} - K_{ic}\hat{i}_{mc}$$

$$\Rightarrow \left(1 + \frac{r_c}{R}\right)C_f \times \frac{d\hat{v}_{c_f}}{dt} = K_{is}\hat{i}_s + K_{ic}\hat{i}_c - K_{is}\hat{i}_{ms} - K_{ic}\hat{i}_{mc} - \left(\frac{1}{R}\right)\hat{v}_{c_f}$$

Where:

$$i_{ps} = i_s - i_{ms} \text{ and } i_{pc} = i_c - i_{mc}$$

$$K_{is} = \frac{2n}{\pi}\frac{I_{ps}}{\sqrt{I_{ps}^2 + I_{pc}^2}} \text{ and } K_{ic} = \frac{2n}{\pi}\frac{I_{pc}}{\sqrt{I_{ps}^2 + I_{pc}^2}}$$

$$\Rightarrow \frac{r_c}{r'_c}C_f \frac{d\hat{v}_{c_f}}{dt} = K_{is}\hat{i}_s + K_{ic}\hat{i}_c - K_{is}\hat{i}_{ms} - K_{ic}\hat{i}_{mc} - \left(\frac{1}{R}\right)\hat{v}_{c_f}$$

$$\frac{d\hat{v}_{c_f}}{dt} = \frac{K_{is}r'_c}{C_f r_c}\hat{i}_s + \frac{K_{ic}r'_c}{C_f r_c}\hat{i}_c - \frac{K_{is}r'_c}{C_f r_c}\hat{i}_{ms} - \frac{K_{ic}r'_c}{C_f r_c}\hat{i}_{mc} - \frac{r'_c}{RC_f r_c}\hat{v}_{c_f}$$

The linearization and perturbation of the output voltage
is provided in Equation 43.

EQUATION 43: LINEARIZATION OF OUTPUT VOLTAGE

$$V_0 + \hat{v}_0 = \frac{2}{\pi} r'_c (I_{sp} + \hat{i}_{sp}) + \left(\frac{r'_c}{r_c}\right)(V_{c_f} + \hat{v}_{c_f})$$

$$\Rightarrow \hat{v}_0 = \frac{2}{\pi} r'_c \hat{i}_{sp} + \left(\frac{r'_c}{r_c}\right)\hat{v}_{c_f}$$

$$\Rightarrow \hat{v}_0 = r'_c (K_{is}\hat{i}_s + K_{ic}\hat{i}_c - K_{is}\hat{i}_{ms} - K_{ic}\hat{i}_{mc}) + \left(\frac{r'_c}{r_c}\right)\hat{v}_{c_f}$$

$$\hat{v}_0 = (K_{is} r'_c \hat{i}_s + K_{ic} r'_c \hat{i}_c - K_{is} r'_c \hat{i}_{ms} - K_{ic} r'_c \hat{i}_{mc}) + \left(\frac{r'_c}{r_c}\right)\hat{v}_{c_f}$$

Equation 32 through Equation 43 are arranged, as
shown in Equation 44.

EQUATION 44: LINEARIZED SMALL SIGNAL MODEL OF LLC RESONANT CONVERTER

$$\frac{d\hat{i}_s}{dt} = -\left(\frac{H_{ip} + r_s}{L_s}\right)\hat{i}_s - \left(\frac{\Omega_s L_s + H_{ic}}{L_s}\right)\hat{i}_c - \frac{1}{L_s}\hat{v}_s + \frac{H_{ip}}{L_s}\hat{i}_{ms} + \frac{H_{ic}}{L_s}\hat{i}_{mc} - \frac{H_{vcf}}{L_s}\hat{v}_{cf} + \frac{K_1}{L_s}\hat{v}_{in} + \frac{K_2}{L_s}\hat{d} - \frac{L_s \omega_0 I_c}{L_s}\hat{\omega}_{sn}$$

$$\frac{d\hat{i}_c}{dt} = \frac{(\Omega_s L_s - G_{ip})}{L_s}\hat{i}_s - \frac{(G_{ic} + r_s)}{L_s}\hat{i}_c - \frac{1}{L_s}\hat{v}_c + \frac{G_{ip}}{L_s}\hat{i}_{ms} + \frac{G_{ic}}{L_s}\hat{i}_{mc} - \frac{G_{vcf}}{L_s}\hat{v}_{cf} + \frac{L_s \omega_0 I_s}{L_s}\hat{\omega}_{sn}$$

$$\frac{d\hat{v}_s}{dt} = \frac{1}{C_s}\hat{i}_s - \frac{C_s \Omega_s}{C_s}\hat{v}_c - \frac{C_s \omega_0 V_c}{C_s}\hat{\omega}_{sn}$$

$$\frac{d\hat{v}_c}{dt} = \frac{1}{C_s}\hat{i}_c + \frac{C_s \Omega_s}{C_s}\hat{v}_s + \frac{C_s \omega_0 V_s}{C_s}\hat{\omega}_{sn}$$

$$\frac{d\hat{i}_{ms}}{dt} = \frac{H_{ip}}{L_m}\hat{i}_s + \frac{H_{ic}}{L_m}\hat{i}_c - \frac{H_{ip}}{L_m}\hat{i}_{ms} - \frac{H_{ic} + L_m \Omega_s}{L_m}\hat{i}_{mc} + \frac{H_{vcf}}{L_m}\hat{v}_{cf} - \frac{L_m I_{mc} \omega_0}{L_m}\hat{\omega}_{sn}$$

$$\frac{d\hat{i}_{mc}}{dt} = \frac{G_{ip}}{L_m}\hat{i}_s + \frac{G_{ic}}{L_m}\hat{i}_c - \frac{(G_{ip} - L_m \Omega_s)}{L_m}\hat{i}_{ms} - \frac{G_{ic}}{L_m}\hat{i}_{mc} + \frac{G_{vcf}}{L_m}\hat{v}_{cf} + \frac{L_m I_{ms} \omega_0}{L_m}\hat{\omega}_{sn}$$

$$\frac{d\hat{V}_{C_f}}{dt} = \frac{K_{is} r'_c}{C_f r_c}\hat{i}_s + \frac{K_{ic} r'_c}{C_f r_c}\hat{i}_c - \frac{K_{is} r'_c}{C_f r_c}\hat{i}_{ms} - \frac{K_{ic} r'_c}{C_f r_c}\hat{i}_{mc} - \frac{r'_c}{RC_f r_c}\hat{v}_{cf}$$

The output equation is:

$$\hat{v}_0 = K_{is} r'_c \hat{i}_s + K_{ic} r'_c \hat{i}_c - K_{is} r'_c \hat{i}_{ms} - K_{ic} r'_c \hat{i}_{mc} + \left(\frac{r'_c}{r_c}\right)\hat{v}_{cf}$$

Formation of State-Space Model

State-space representation is a mathematical model of a physical system as a set of input, output and state variables, related by first order differential equations.

Additionally, if the dynamic system is linear and time invariant, the differential and algebraic equations may be written in matrix form.

The state-space representation (known as time domain approach) provides a convenient and compact way to model and analyze systems with multiple inputs and outputs.

Equation 45 provides the state-space representation of the LLC resonant converter.

EQUATION 45: STATE-SPACE MODEL OF LLC RESONANT CONVERTER

$$\frac{d\hat{x}}{dt} = A\hat{x} + B\hat{u}$$

$$\hat{y} = C\hat{x} + D\hat{u}$$

Where:

$\hat{x} = \left(\hat{i}_s \ \hat{i}_c \ \hat{v}_s \ \hat{v}_c \ \hat{i}_{ms} \ \hat{i}_{mc} \ \hat{v}_{c_f}\right)^T$ States of the system

$\hat{u} = (\hat{f}_{sn} \ or \ \hat{\omega}_{sn})$ Control inputs and all other disturbance inputs are ignored

$\hat{y} = (\hat{v}_0)$ Output

$$A = \begin{bmatrix} -\dfrac{H_{ip}+r_s}{L_s} & -\dfrac{(\Omega_s L_s + H_{ic})}{L_s} & -\dfrac{1}{L_s} & 0 & \dfrac{H_{ip}}{L_s} & \dfrac{H_{ic}}{L_s} & -\dfrac{H_{vcf}}{L_s} \\[3mm] \dfrac{(\Omega_s L_s - G_{ip})}{L_s} & -\dfrac{G_{ic}+r_s}{L_s} & 0 & -\dfrac{1}{L_s} & \dfrac{G_{ip}}{L_s} & \dfrac{G_{ic}}{L_s} & -\dfrac{G_{vcf}}{L_s} \\[3mm] \dfrac{1}{C_s} & 0 & 0 & -\dfrac{C_s \Omega_s}{C_s} & 0 & 0 & 0 \\[3mm] 0 & \dfrac{1}{C_s} & \dfrac{C_s \Omega_s}{C_s} & 0 & 0 & 0 & 0 \\[3mm] \dfrac{H_{ip}}{L_m} & \dfrac{H_{ic}}{L_m} & 0 & 0 & -\dfrac{H_{ip}}{L_m} & -\dfrac{H_{ic}+L_m \Omega_s}{L_m} & \dfrac{H_{vcf}}{L_m} \\[3mm] \dfrac{G_{ip}}{L_m} & \dfrac{G_{ic}}{L_m} & 0 & 0 & -\dfrac{G_{ip}-L_m \Omega_s}{L_m} & -\dfrac{G_{ic}}{L_m} & \dfrac{G_{vcf}}{L_m} \\[3mm] \dfrac{K_{is} r'_c}{C_f r_c} & \dfrac{K_{ic} r'_c}{C_f r_c} & 0 & 0 & -\dfrac{K_{is} r'_c}{C_f r_c} & -\dfrac{K_{ic} r'_c}{C_f r_c} & -\dfrac{r'_c}{RC_f r_c} \end{bmatrix}$$

$$B = ((-\omega_0 I_c) \ (\omega_0 I_s) \ (-\omega_0 V_c) \ (\omega_0 V_s) \ (-\omega_0 I_{mc}) \ (\omega_0 I_{ms}) \ 0)^T$$

$$C = \left[(K_{is} r'_c) \ (K_{ic} r'_c) \ (0) \ (0) \ (-K_{is} r'_c) \ (-K_{ic} r'_c) \ \left(\frac{r'_c}{r_c}\right)\right]$$

$$D = 0$$

For the linearized system, the required control-to-output voltage transfer function is:

$$\frac{\hat{v}_0}{\hat{\omega}_{sn}} = C(SI-A)^{-1}B + D = G_p(s)$$

HARDWARE DESIGN SPECIFICATIONS

Series resonant inductor (L_s) = 62 μH

Series resonant capacitance (C_s) = 9.4 nF

Magnetizing inductor (L_m) = 268 μH

Input voltage (V_{in}) = 400V (DC)

Output filter capacitance (C_f) = 2000 μF

Output power = 200W

Switching frequency (f_s) = 200 kHz

DCR of resonant inductor (r_s) = 15 mΩ

ESR of output capacitor (r_c) = 15 mΩ

Secondary MOS resistor (r_d) = 0.725 mΩ

Equation 45 can be solved using MATLAB® to obtain the control-to-output (plant) transfer function, `sys = ss(A, B, C, D)`. The `ss` command arranges the `A`, `B`, `C` and `D` matrices in a state-space model. The $G_p(s)$ = `tf(sys)` command gives the transfer function of the system, where `sys` indicates the system. The plant transfer function order is reduced by neglecting the poles and zeros having frequency higher than the switching frequency. The reduced order plant transfer function ($G_p(s)$), along with the design values, are shown in Equation 46.

EQUATION 46: PLANT TRANSFER FUNCTION

$$G_p(s) = \frac{40311827883 \times (s + 1.98 \times 10^5) \times (s - 6.711 \times 10^5)}{(s^2 + 4.102 \times 10^4 s + 7.937 \times 10^8) \times (s^2 + 2.697 \times 10^5 s + 1.05 \times 10^{12})}$$

$$G_p(s) = \frac{6.4275 \times \left[\dfrac{s}{1.98 \times 10^5} + 1\right] \times \left[\dfrac{s}{6.711 \times 10^5} - 1\right]}{\left[\dfrac{s^2}{7.937 \times 10^8} + \dfrac{4.102 \times 10^4}{7.937 \times 10^8}s + 1\right] \times \left[\dfrac{s^2}{1.05 \times 10^{12}} + \dfrac{2.697 \times 10^5}{1.05 \times 10^{12}}s + 1\right]}$$

The general form of $G_p(s)$ is shown in Equation 47.

EQUATION 47: GENERALIZED FORM OF PLANT TRANSFER FUNCTION

$$G_p(s) = \frac{G_{po}\left(1 + \dfrac{s}{\omega_{esr}}\right) \times \left(\dfrac{s}{\omega_{RHP}} - 1\right)}{\left(\dfrac{s^2}{\omega_{p1}^2} + \dfrac{s}{Q_1 \times \omega_{p1}} + 1\right) \times \left(\dfrac{s^2}{\omega_{p2}^2} + \dfrac{s}{Q_2 \times \omega_{p2}} + 1\right)}$$

The `[p, z] = pzmap (Gp(s))` command gives the poles and zeros of the plant transfer function. Figure 7 illustrates the pole-zero plot for the $G_p(s)$, which is obtained from the MATLAB command, `pzmap (Gp(s))`. Figure 7 shows dominant poles and zero of Equation 46, excluding RHP zero and high-frequency poles. Figure 8 illustrates the Bode plot obtained using MATLAB for detail plant transfer function and reduced order plant transfer function.

FIGURE 7: **POLE-ZERO MAP OF PLANT TRANSFER FUNCTION**
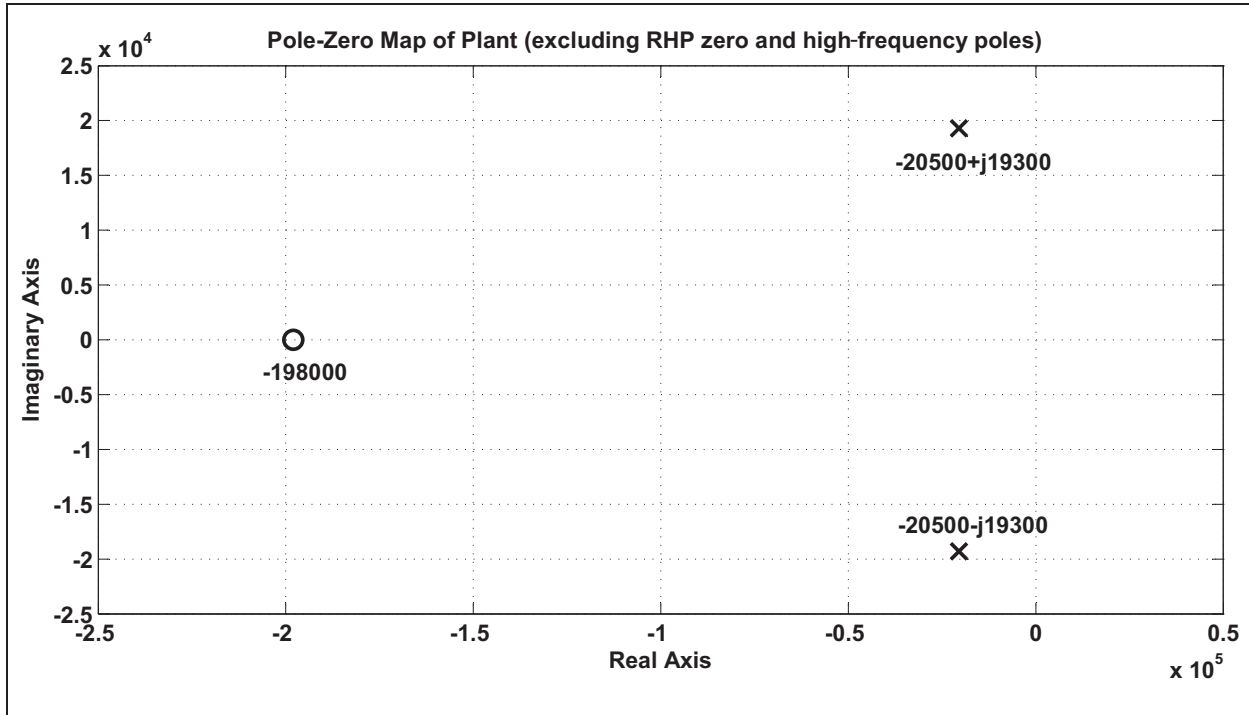
FIGURE 8: **SIMULATED BODE DIAGRAM OF PLANT TRANSFER FUNCTION**

AN1477
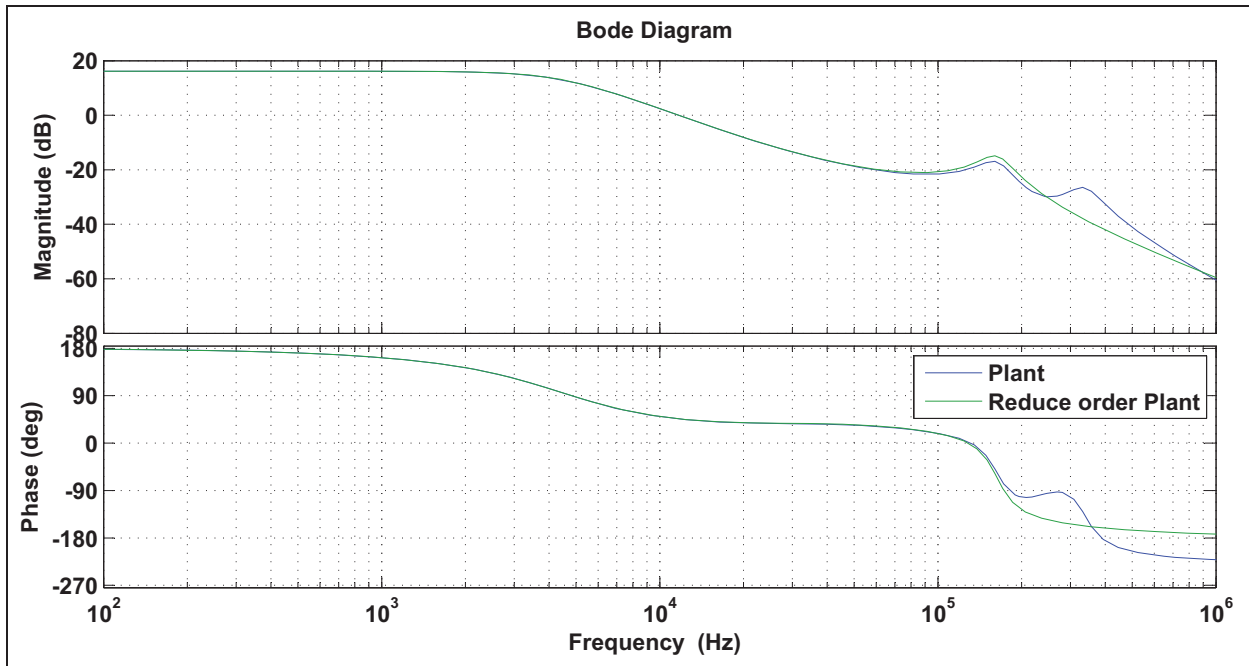
Digital Compensator Design for LLC Resonant Converter

The plant model is derived as shown in Equation 46. In order to attain the desired gain margin, phase margin and crossover frequency, a digital 2P2Z compensator is designed. The digital 2P2Z compensator is derived using the design by emulation or digital redesign approach.

In this method, an analog compensator is first designed in the continuous time domain and then converted to discrete time domain using bilinear or tustin transformation. Figure 9 illustrates the block diagram of the LLC resonant converter with a digital compensator.

After deriving a plant model, the controller design process starts with derivation of open-loop gain to get the desired phase margin and crossover frequency for the specified performance of the closed-loop system. The block diagram in Figure 10 shows the system in continuous time domain. The block diagram of Figure 10 can be simplified in terms of per unit system, using $1/V_{base}$ gain in the forward path of the closed-loop system, where $V_{base} = 3.3/K_S$. Figure 11 shows the per unit block diagram. V_{base} is an essential gain to consider while designing the controller. Figure 10 and Figure 11 are used only to design the controller in continuous time domain. In the digital implementation, the controller output is period instead of normalized frequency.

FIGURE 9: BLOCK DIAGRAM OF LLC RESONANT CONVERTER
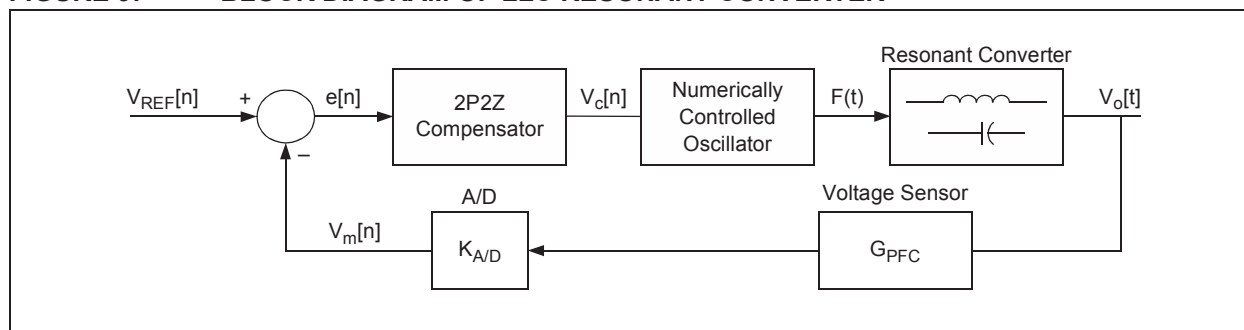
FIGURE 10: CLOSED-LOOP CONTROL BLOCK DIAGRAM IN CONTINUOUS TIME DOMAIN
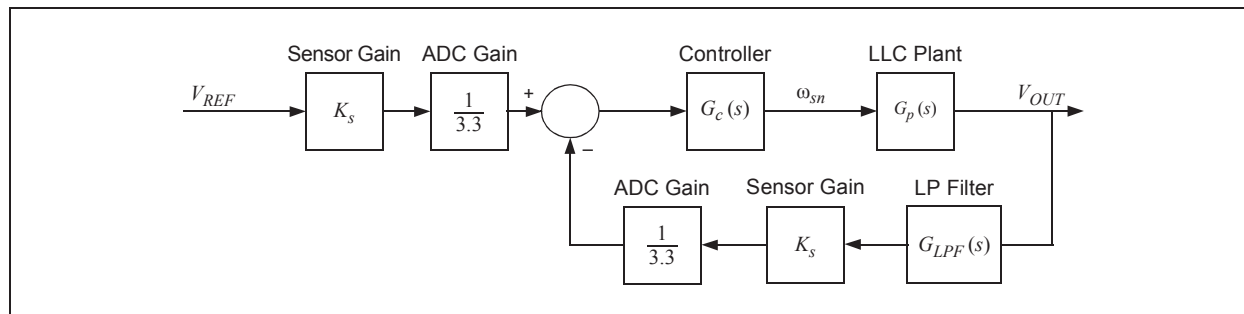
FIGURE 11: SIMPLIFIED CLOSED-LOOP CONTROL BLOCK DIAGRAM IN PER UNIT INCLUDING V_{base}
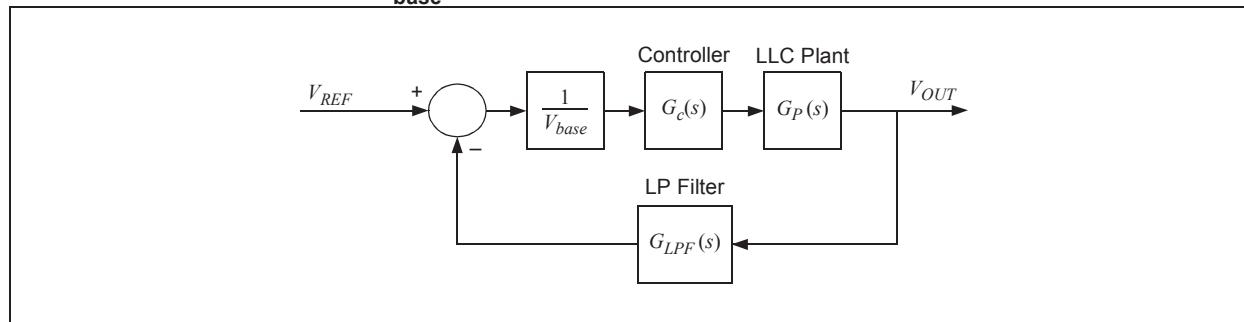
As seen from Equation 47, plant transfer function consists of an ESR zero and a pair of dominant complex poles. In order to compensate for the effect of ESR zero (increased high-frequency gain, and thereby, increased ripple), a pole (ω_p) is included in the compensator. In order to minimize the steady-state error, an integrator (K_c) is also added to the compensator.

Furthermore, in order to compensate for the effect of the complex dominant poles (reduction in system damping, and hence, increased overshoots and settling time), two zeros, $(s + \alpha + j\beta)$ and $(s + \alpha - j\beta)$, are added.

Effectively, the system will have a 2-Pole 2-Zero (2P2Z) compensator in continuous domain, as shown in Equation 48.

EQUATION 48:   COMPENSATOR $G_C(s)$ IN CONTINUOUS TIME DOMAIN

$$G_c(s) = \frac{K_c \times \left(\frac{s^2}{\omega_z^2} + \frac{s}{Q_c \times \omega_z} + 1\right)}{s \times \left(\frac{s}{\omega_p} + 1\right)}$$

$$G_c(s) = \frac{K_c/\omega_z^2 \times (s + \alpha + j\beta) \times (s + \alpha - j\beta)}{s \times \left(\frac{s}{\omega_p} + 1\right)}$$

One of the digital compensator poles ($\omega_p = 2\pi f_p$) is placed at f_p to cancel the ESR zero due to output filter capacitor ESR ($f_{esr} = \omega_{esr}/2\pi$).

K_c represents the integral gain of the compensator and is adjusted to achieve the desired crossover frequency of the system.

A pair of complex zeros of the compensator, on the complex s-plane, is at $s_1 = -\alpha + j\beta$ and $s_2 = -\alpha - j\beta$. The compensator zero frequency magnitude (ω_z) is $2\pi f_z$. The frequency (f_z) is chosen slightly below or equal to the corner frequency of the dominant resonant poles (ω_{p1}) to provide the necessary phase lead. The compensator quality factor (Q_c) is chosen to be comparable, or equal to, the dominant complex pole pair quality factor (Q_1) of the plant transfer function at the maximum load current. For this analysis, computational delay is ignored. The computational delay is, however, considered in the model loop gain while comparing the model predicted loop gain with experimentally obtained loop gain.

If the desired crossover frequency is denoted as (f_c), then $\omega_c = j2\pi f_c$.

At crossover frequency, the loop gain of the system should be zero dB or one on linear scale, as shown in Equation 49.

EQUATION 49:   COMPENSATOR GAIN CALCULATION

$$G_p(s)\Big|_{s = \omega_c} \times G_c(s)\Big|_{s = \omega_c} = 1$$

The required gain of the compensator is:

$$K_c = \frac{1}{G_p(s)\Big|_{s = \omega_c}} \times \frac{1}{G_c(s)\Big|_{s = \omega_c}} \times V_{base}$$

The compensator first pole (ω_p) is placed at 198k rad/sec and the complex pair of zeros is placed at 25k rad/sec. The resulting compensator for a crossover frequency of 10.5 kHz is shown in Equation 50.
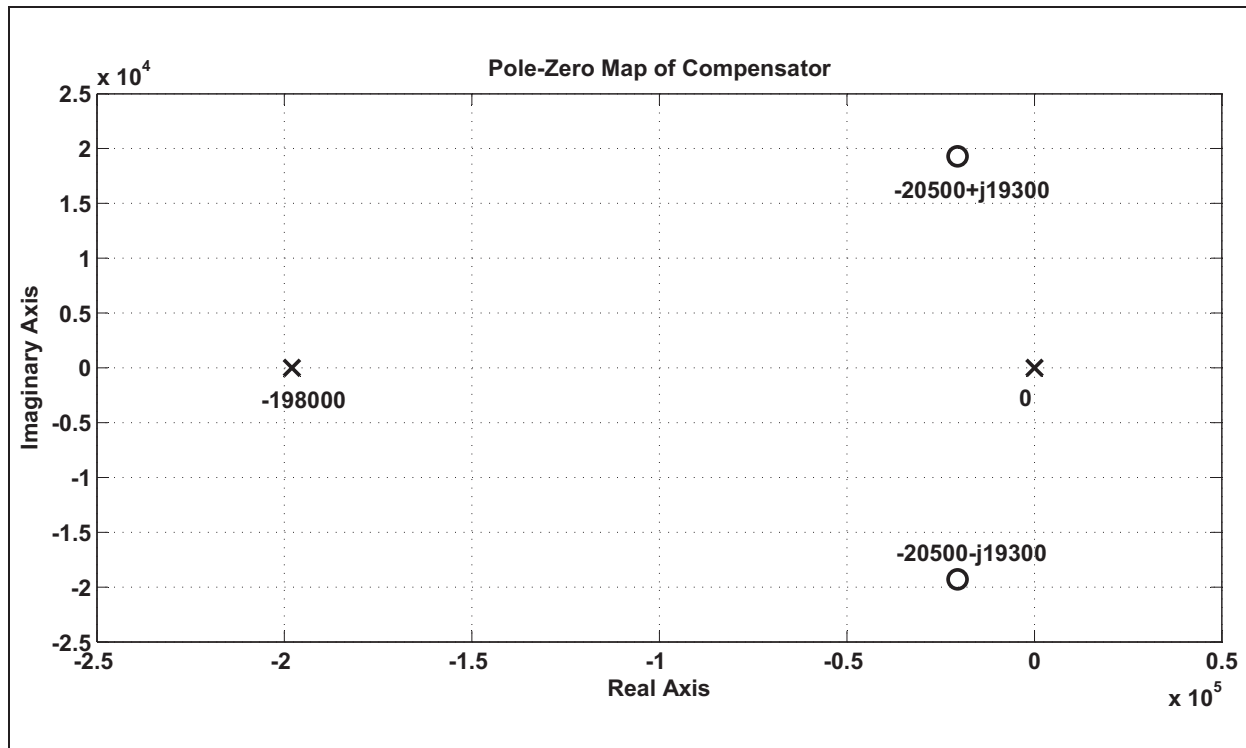
EQUATION 50:   COMPENSATOR TRANSFER FUNCTION

$$G_c(s) = \frac{36.97 \times (s^2 + 3.714 \times 10^4 s + 6.292 \times 10^8)}{s \times (s + 1.98 \times 10^5)}$$
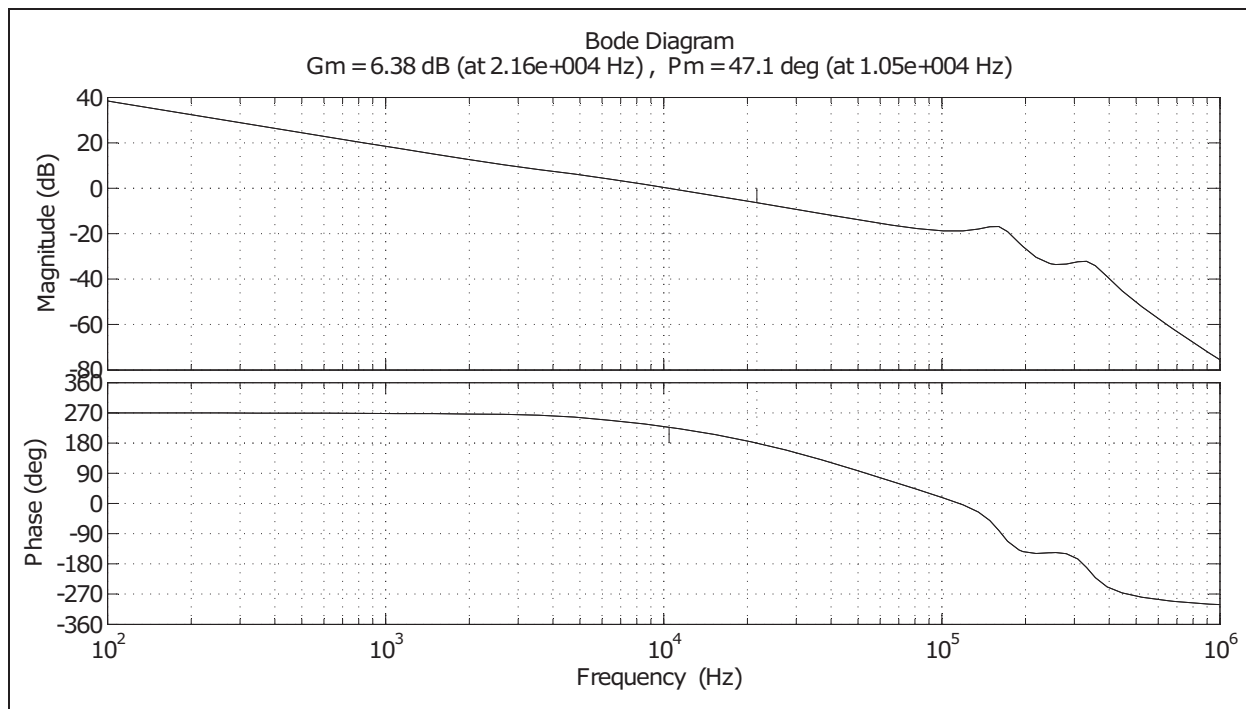
The $[p, z]$ = $pzmap$ $(G_c(s))$ command gives the poles and zeros of the compensator. Figure 12 illustrates the pole-zero plot for a G_c.

Figure 13 illustrates the simulated Bode plot of loop gain with designed compensator.

FIGURE 12: POLE-ZERO MAP OF COMPENSATOR

Pole-Zero Map of Compensator

-20500+j19300

-198000

0

-20500-j19300

FIGURE 13: SIMULATION BODE DIAGRAM OF LOOP GAIN

Bode Diagram
Gm = 6.38 dB (at 2.16e+004 Hz), Pm = 47.1 deg (at 1.05e+004 Hz)

The discrete compensator transfer function (G_{c_d}) is obtained using the tustin or bilinear transformation with a sampling frequency of 200 kHz, as shown in Equation 51. Another method to design and implement the controller is discussed in the **"Appendix"** section.

EQUATION 51: COMPENSATOR TRANSFER FUNCTION IN DISCRETE DOMAIN

$$G_{c\_d}(z) = \frac{27.12z^2 - 49.26z + 22.53}{z^2 - 1.338z + 0.3378}$$

Figure 14, Figure 15 and Figure 16 show the comparison of simulated and measured loop gain plots for 100%, 50% and 10% load conditions, respectively. A practical delay of 8.55 µs is produced due to digital compensator implementation, which is added in simulation loop gain plots.

FIGURE 14: COMPARISON OF SIMULATION AND MEASURED LOOP GAIN FOR FULL LOAD
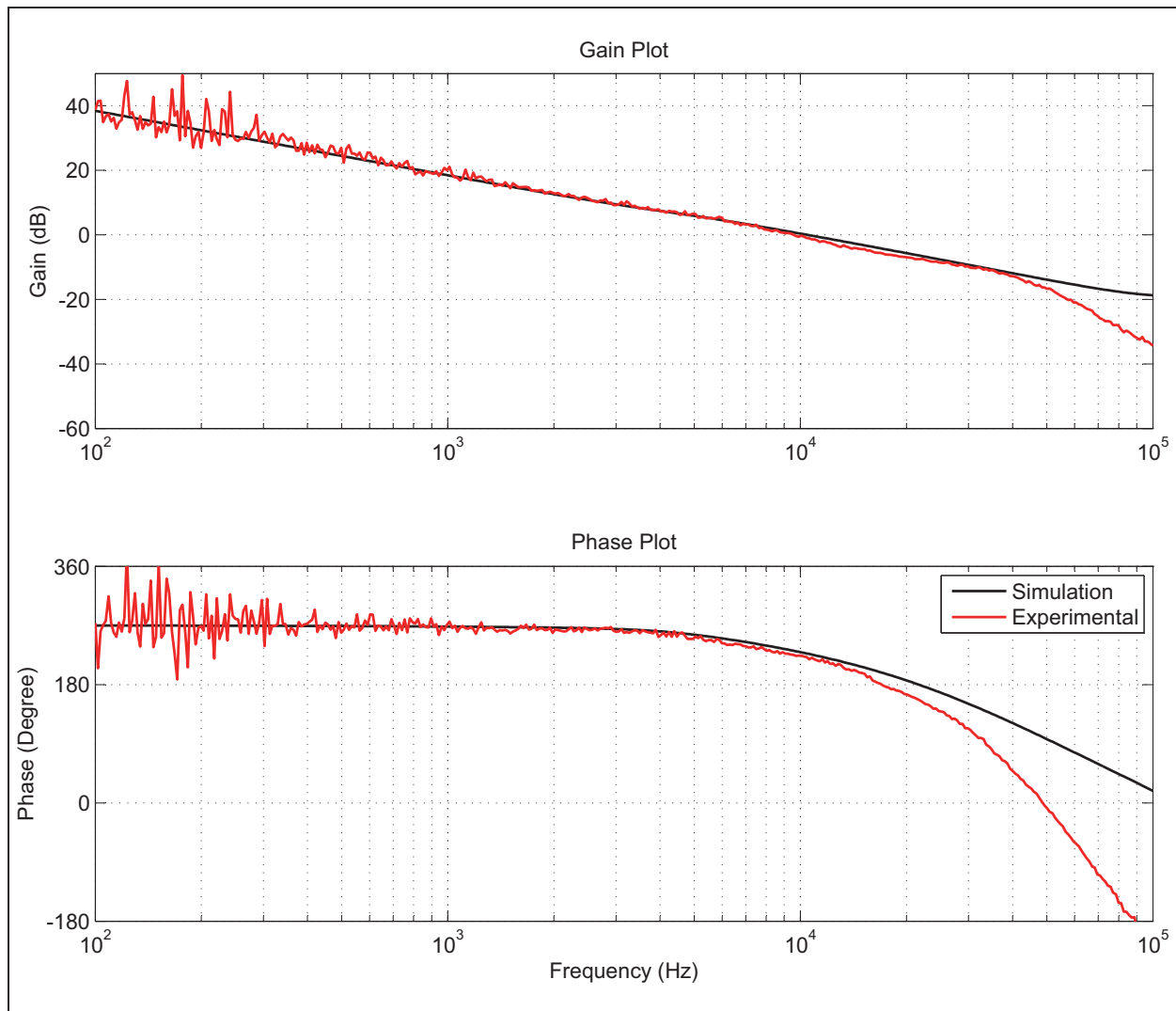
FIGURE 15: **COMPARISON OF SIMULATION AND MEASURED LOOP GAIN FOR 50% LOAD**
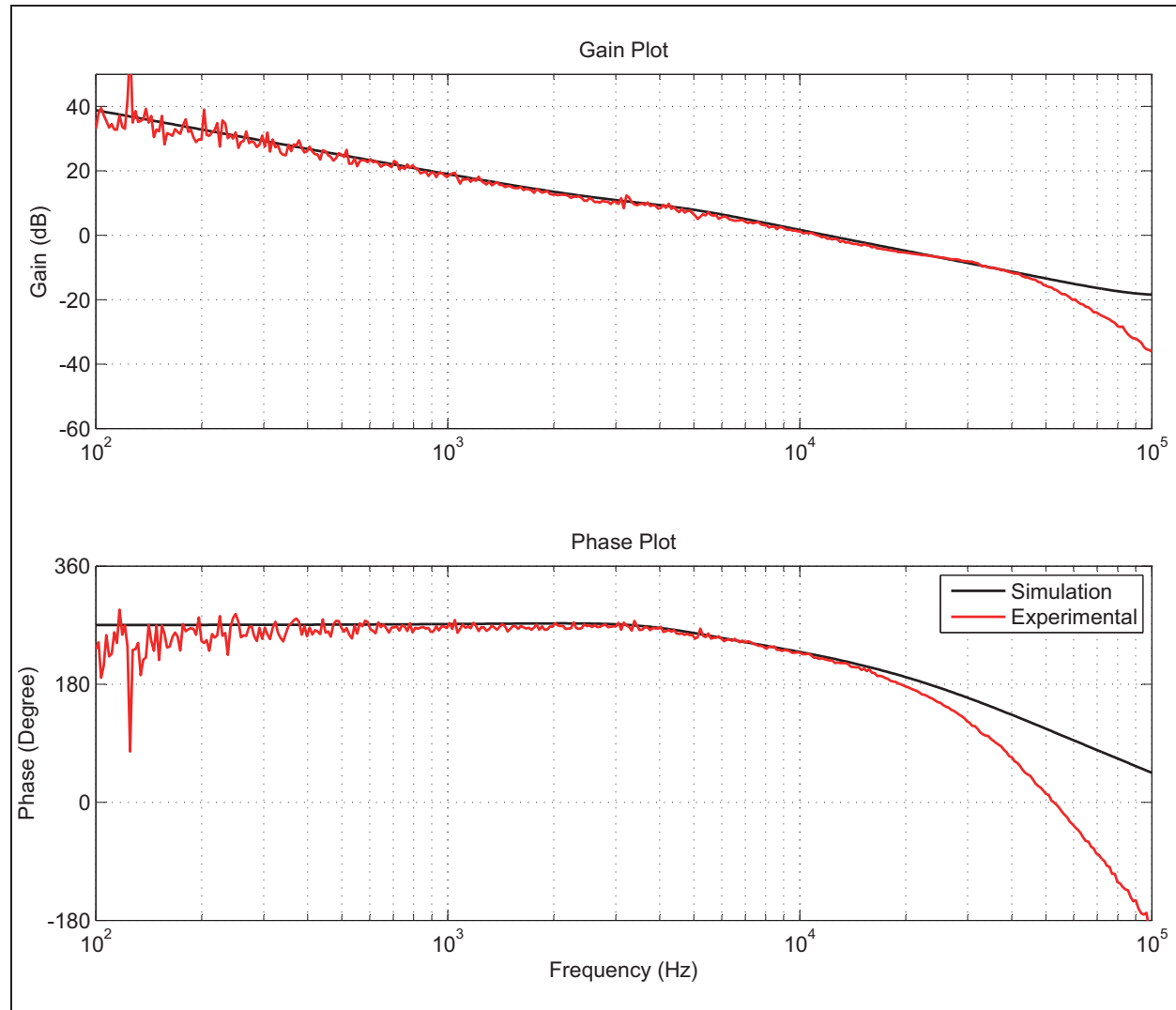
FIGURE 16: COMPARISON OF SIMULATION AND MEASURED LOOP GAIN FOR 10% LOAD
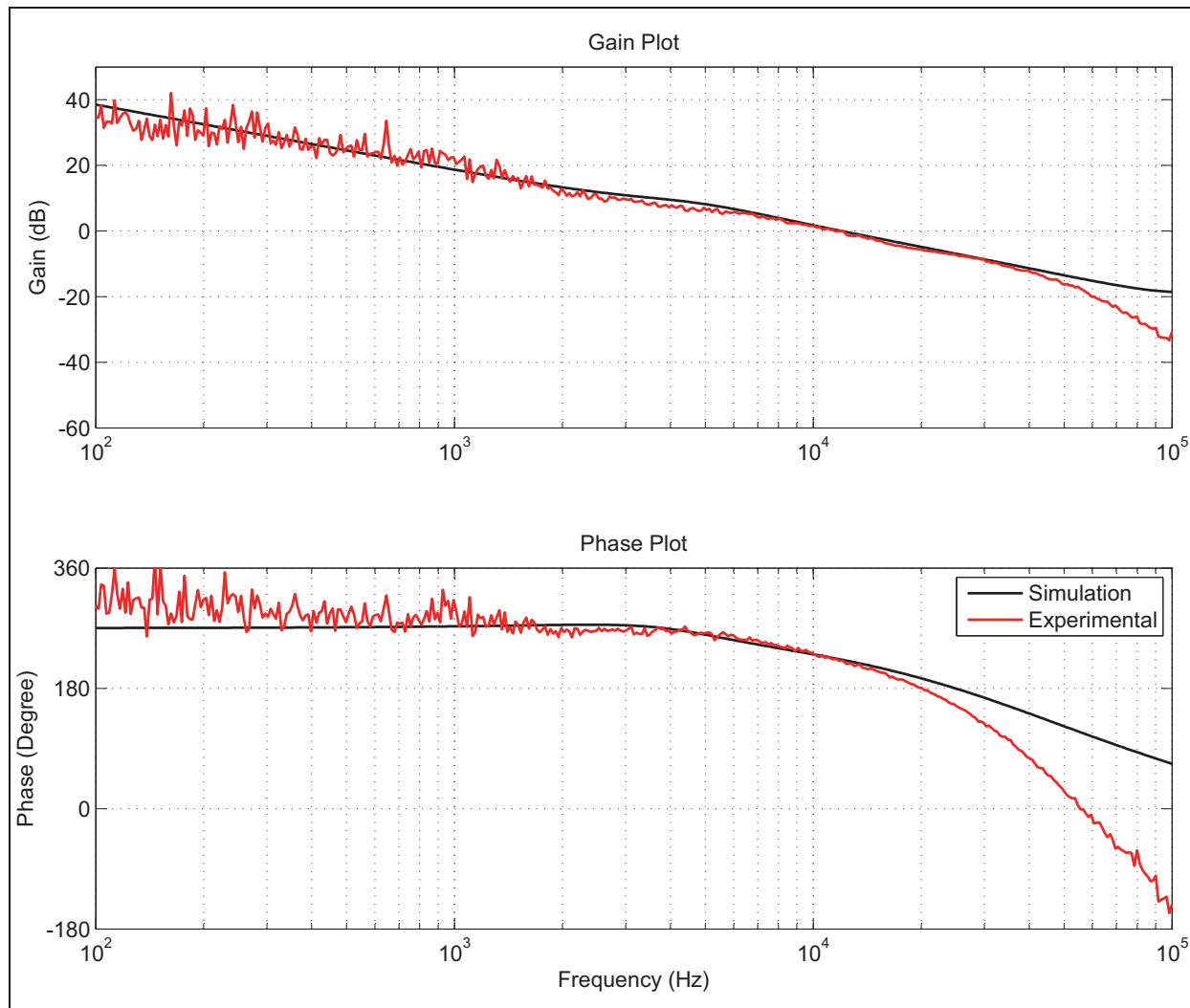
Table 1 shows the comparison of measured and simulated phase margin and crossover frequency for 100%, 50% and 10% load conditions.

TABLE 1: COMPARISON OF SIMULATION AND MEASURED CROSSOVER FREQUENCY AND PHASE MARGIN FOR DIFFERENT LOADS

Load	Crossover Frequency (Hz)		Phase Margin (Degree)	
	Simulation	Experimental	Simulation	Experimental
10%	11489	12000	44.03	42.9
50%	11232	11900	39.43	41
100%	9582	10500	45.11	47.1

AN1477

CONCLUSION

Pulse Frequency Modulated LLC resonant converter plant transfer function is derived by employing the EDF. A digital compensator is designed to get an open-loop gain of a closed-loop system with a very high crossover frequency of ~10 kHz and a phase margin of ~45 degrees. The hardware results are in conformity to the developed analytical model and also meet the target specifications.

APPENDIX

Another commonly used design methodology involves a compensator designed in a continuous time domain, precluding the effects of an ADC, sensor and PWM generator. However, while implementing the digital compensator, the gains due to these blocks are evaluated and an inverse gain is multiplied to the compensator to nullify their effect. This way, the implemented loop gain is equivalent to the designed loop gain in continuous time domain. In other words, while implementing the digital controller, calculate the combined gain offered by the ADC gain, sensor gain and PWM gain, and multiply the inverse of the gain with the continuous time domain equation. Then, convert it in a discrete time domain controller ($G'_c(s)$) using bilinear or tustin transformation. Compensator $G'_c(s)$ is shown in Equation 52. Calculation of compensator gain, K'_c, is given in Equation 53. Figure 17 shows a block diagram that explains this method. Here, controller $G'_c(s)$ is multiplied with gain constant, K, which is derived in Equation 54.

EQUATION 52: COMPENSATOR $G'_C(s)$ IN CONTINUOUS TIME DOMAIN

$$G'_c(s) = \frac{K'_c \times \left(\dfrac{s^2}{\omega_z^2} + \dfrac{s}{Q_c \times \omega_z} + 1\right)}{s \times \left(\dfrac{s}{\omega_p} + 1\right)}$$

$$G'_c(s) = \frac{K'_c / \omega_z^2 \times (s + \alpha + j\beta) \times (s + \alpha - j\beta)}{s \times \left(\dfrac{s}{\omega_p} + 1\right)}$$

EQUATION 53: COMPENSATOR GAIN K'_C CALCULATION

$$G_p(s)\Big|_{s = \omega_c} \times G'_c(s)\Big|_{s = \omega_c} = 1$$

The required gain of the compensator is:

$$K'_c = \frac{1}{G_p(s)\Big|_{s = \omega_c}} \times \frac{1}{G'_c(s)\Big|_{s = \omega_c}}$$

EQUATION 54: GAIN CONSTANT K MULTIPLIED WITH CONTROLLER

$$K = \frac{3.3}{K_s} \times \frac{P_{base}}{2^n}$$

Where:

n = ADC bits

P_{base} = Period corresponds to the base frequency of LLC converter

FIGURE 17: SIMPLIFIED CLOSED-LOOP CONTROL BLOCK DIAGRAM
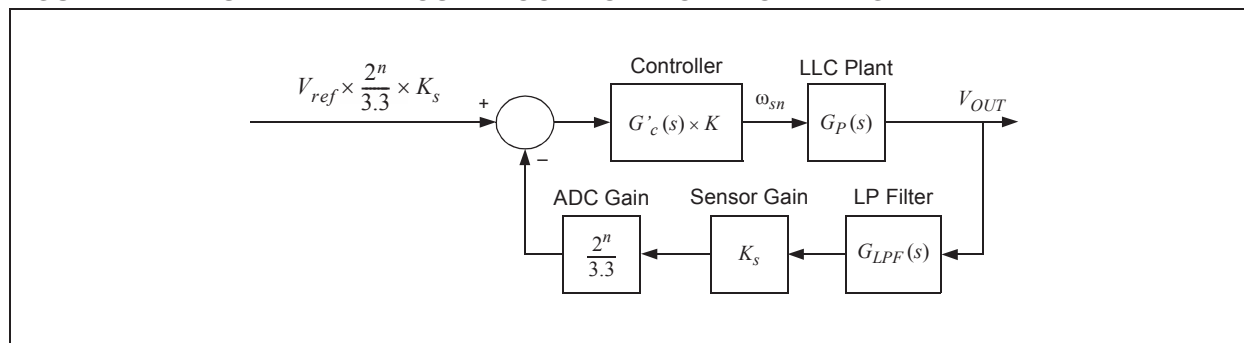
REFERENCES

- *"Topology Investigation for Front End DC/DC Power Conversion for Distributed Power Systems"*, by Bo Yang, Dissertation, Virginia Polytechnic Institute and State University, 2003.
- *"Small-Signal Analysis for LLC Resonant Converter"*, by Bo Yang and F.C. Lee, CPES Seminar, 2003, S7.3, Pages: 144-149.
- *"Small-Signal Modeling of Series and Parallel Resonant Converters"*, by Yang, E.X.; Lee, F.C.; Jovanovich, M.M., Applied Power Electronics Conference and Exposition, 1992. APEC' 92. Conference Proceedings 1992, Seventh Annual, 1992, Page(s): 785-792.
- *"Approximate Small-Signal Analysis of the Series and the Parallel Resonant Converters"*, by Vorperian, V., Power Electronics, IEEE Transactions on, Vol. 4, Issue 1, January 1989, Page(s): 15-24.
- *"DC/DC LLC Reference Design Using the dsPIC® DSC"* (AN1336)

LIST OF PARAMETERS

TABLE 2:   LIST OF PARAMETERS AND DESCRIPTION

Parameter	Description
I_r	Resonant tank current
V_c	Resonant tank capacitor voltage
I_m	Magnetizing current
V_{cf}	Output capacitor voltage
v'_{cf}	Reflected output capacitor voltage on primary side
I_{sp}	Transformer secondary current
I_{is}	Sine component of resonant tank current
I_{ic}	Cosine component of resonant tank current
V_{cs}	Sine component of resonant tank capacitor voltage
V_{cc}	Cosine component of resonant tank capacitor voltage
I_{ms}	Sine component of magnetizing current
I_{mc}	Cosine component of magnetizing current
I_{ss}	Sine component of transformer secondary current
I_{sc}	Cosine component of transformer secondary current
V_{es}	Sine component of half-bridge inverter output voltage
V_{ec}	Cosine component of half-bridge inverter output voltage
I_{ps}	Sine component of transformer primary current
I_{pc}	Cosine component of transformer primary current
I_{pp}	Total primary current of transformer
V_{ps}	Sine component of transformer primary voltage
V_{pc}	Cosine component of transformer primary voltage
n	Transformer turns ratio

NOTES:

Note the following details of the code protection feature on Microchip devices:

• Microchip products meet the specification contained in their particular Microchip Data Sheet.

• Microchip believes that its family of products is one of the most secure families of its kind on the market today, when used in the intended manner and under normal conditions.

• There are dishonest and possibly illegal methods used to breach the code protection feature. All of these methods, to our knowledge, require using the Microchip products in a manner outside the operating specifications contained in Microchip's Data Sheets. Most likely, the person doing so is engaged in theft of intellectual property.

• Microchip is willing to work with the customer who is concerned about the integrity of their code.

• Neither Microchip nor any other semiconductor manufacturer can guarantee the security of their code. Code protection does not mean that we are guaranteeing the product as "unbreakable."

Code protection is constantly evolving. We at Microchip are committed to continuously improving the code protection features of our products. Attempts to break Microchip's code protection feature may be a violation of the Digital Millennium Copyright Act. If such acts allow unauthorized access to your software or other copyrighted work, you may have a right to sue for relief under that Act.

QUALITY MANAGEMENT SYSTEM

CERTIFIED BY DNV

═ ISO/TS 16949 ═

Worldwide Sales and Service

AMERICAS

Corporate Office
2355 West Chandler Blvd.
Chandler, AZ 85224-6199
Tel: 480-792-7200
Fax: 480-792-7277
Technical Support:
http://www.microchip.com/
support
Web Address:
www.microchip.com

Atlanta
Duluth, GA
Tel: 678-957-9614
Fax: 678-957-1455

Austin, TX
Tel: 512-257-3370

Boston
Westborough, MA
Tel: 774-760-0087
Fax: 774-760-0088

Chicago
Itasca, IL
Tel: 630-285-0071
Fax: 630-285-0075

Dallas
Addison, TX
Tel: 972-818-7423
Fax: 972-818-2924

Detroit
Novi, MI
Tel: 248-848-4000

Houston, TX
Tel: 281-894-5983

Indianapolis
Noblesville, IN
Tel: 317-773-8323
Fax: 317-773-5453
Tel: 317-536-2380

Los Angeles
Mission Viejo, CA
Tel: 949-462-9523
Fax: 949-462-9608
Tel: 951-273-7800

Raleigh, NC
Tel: 919-844-7510

New York, NY
Tel: 631-435-6000

San Jose, CA
Tel: 408-735-9110
Tel: 408-436-4270

Canada - Toronto
Tel: 905-695-1980
Fax: 905-695-2078

ASIA/PACIFIC

Australia - Sydney
Tel: 61-2-9868-6733

China - Beijing
Tel: 86-10-8569-7000

China - Chengdu
Tel: 86-28-8665-5511

China - Chongqing
Tel: 86-23-8980-9588

China - Dongguan
Tel: 86-769-8702-9880

China - Guangzhou
Tel: 86-20-8755-8029

China - Hangzhou
Tel: 86-571-8792-8115

China - Hong Kong SAR
Tel: 852-2943-5100

China - Nanjing
Tel: 86-25-8473-2460

China - Qingdao
Tel: 86-532-8502-7355

China - Shanghai
Tel: 86-21-3326-8000

China - Shenyang
Tel: 86-24-2334-2829

China - Shenzhen
Tel: 86-755-8864-2200

China - Suzhou
Tel: 86-186-6233-1526

China - Wuhan
Tel: 86-27-5980-5300

China - Xian
Tel: 86-29-8833-7252

China - Xiamen
Tel: 86-592-2388138

China - Zhuhai
Tel: 86-756-3210040

ASIA/PACIFIC

India - Bangalore
Tel: 91-80-3090-4444

India - New Delhi
Tel: 91-11-4160-8631

India - Pune
Tel: 91-20-4121-0141

Japan - Osaka
Tel: 81-6-6152-7160

Japan - Tokyo
Tel: 81-3-6880- 3770

Korea - Daegu
Tel: 82-53-744-4301

Korea - Seoul
Tel: 82-2-554-7200

Malaysia - Kuala Lumpur
Tel: 60-3-7651-7906

Malaysia - Penang
Tel: 60-4-227-8870

Philippines - Manila
Tel: 63-2-634-9065

Singapore
Tel: 65-6334-8870

Taiwan - Hsin Chu
Tel: 886-3-577-8366

Taiwan - Kaohsiung
Tel: 886-7-213-7830

Taiwan - Taipei
Tel: 886-2-2508-8600

Thailand - Bangkok
Tel: 66-2-694-1351

Vietnam - Ho Chi Minh
Tel: 84-28-5448-2100

EUROPE

Austria - Wels
Tel: 43-7242-2244-39
Fax: 43-7242-2244-393

Denmark - Copenhagen
Tel: 45-4450-2828
Fax: 45-4485-2829

Finland - Espoo
Tel: 358-9-4520-820

France - Paris
Tel: 33-1-69-53-63-20
Fax: 33-1-69-30-90-79

Germany - Garching
Tel: 49-8931-9700

Germany - Haan
Tel: 49-2129-3766400

Germany - Heilbronn
Tel: 49-7131-67-3636

Germany - Karlsruhe
Tel: 49-721-625370

Germany - Munich
Tel: 49-89-627-144-0
Fax: 49-89-627-144-44

Germany - Rosenheim
Tel: 49-8031-354-560

Israel - Ra'anana
Tel: 972-9-744-7705

Italy - Milan
Tel: 39-0331-742611
Fax: 39-0331-466781

Italy - Padova
Tel: 39-049-7625286

Netherlands - Drunen
Tel: 31-416-690399
Fax: 31-416-690340

Norway - Trondheim
Tel: 47-7288-4388

Poland - Warsaw
Tel: 48-22-3325737

Romania - Bucharest
Tel: 40-21-407-87-50

Spain - Madrid
Tel: 34-91-708-08-90
Fax: 34-91-708-08-91

Sweden - Gothenberg
Tel: 46-31-704-60-40

Sweden - Stockholm
Tel: 46-8-5090-4654

UK - Wokingham
Tel: 44-118-921-5800
Fax: 44-118-921-5820